

1N-33
47530
P-100

NASA Contractor Report 189057

Design of a Fast Computer-Based Partial Discharge Diagnostic System

Jose R. Oliva, G.G. Karady and Stan Domitz

GRANT NAG3-1139

August 1991

(NASA-CR-189057) DESIGN OF A FAST
COMPUTER-BASED PARTIAL DISCHARGE DIAGNOSTIC
SYSTEM Final Report (Arizona State Univ.)
100 p

CSCL 09A

N72-11272

Unclas

G3/33 0047530



ABSTRACT

Partial discharges cause progressive deterioration of insulating materials working in high voltage conditions and may lead ultimately to insulator failure. Experimental findings indicate that deterioration increases with the number of discharges and is consequently proportional to the magnitude and frequency of the applied voltage. In order to obtain a better understanding of the mechanisms of deterioration produced by partial discharges, instrumentation capable of individual pulse resolution is required. A new computer-based partial discharge detection system was designed and constructed to conduct long duration tests on sample capacitors. This system is capable of recording large number of pulses without dead time and producing valuable information related to amplitude, polarity and charge content of the discharges. The operation of the system is automatic and no human supervision is required during the testing stage. Ceramic capacitors were tested at high voltage in long duration tests. The results obtained indicate that the charge content of partial discharges shifts toward higher levels of charge as the level of deterioration in the capacitor increases.

TABLE OF CONTENTS

	Page
LIST OF TABLES.....	vii
LIST OF FIGURES.....	viii
CHAPTER	
1 INTRODUCTION	1
1.1 Background	1
1.2 Problem.....	4
1.3 Purpose.....	7
2 LITERATURE REVIEW	9
2.1 Introduction.....	9
2.2 Detection networks.....	10
2.3 Pulse processing instruments	19
2.4 Computer - based partial discharge diagnostic systems.....	21
2.5 Conclusions.....	25
3 DESCRIPTION OF THE SYSTEM.....	27
3.1 Introduction.....	27
3.2 General description	27
3.3 Data acquisition system theory	44
3.4 Operation of the partial discharge acquisition and analysis system proposed	49
3.5 Description of the instruments.....	50
3.6 Calibration.....	64
4 EXPERIMENTAL VERIFICATION.....	72
4.1 General.....	72
4.2 Tests using a pulse generator	72
4.3 Testing of sample capacitors.....	76

CHAPTER	Page
4.4 Conclusions from the measured results.....	84
5 CONCLUSIONS AND RECOMMENDATIONS FOR FUTURE WORK.....	85
REFERENCES	89
APPENDIX	
A Photograph of PD Data Acquisition system	93
B Electrical Specifications of TEKTRONIX RTD 710.....	95
C Electrical Specifications of TEKTRONIX FDC 9503.....	99

LIST OF TABLES

Table	Page
3.1 TEKTRONIX RTD 710 Waveform Digitizer	
Electrical Specifications.....	51
3.2 TEKTRONIX FDC 9503 Fast Data Cache	
Electrical Specifications.....	55

LIST OF FIGURES

Figure	Page
1.1 Block diagram of PD detection system	7
2.1 RCL network.....	12
2.2 Discriminating circuit.....	13
2.3 Real dielectric representation.....	15
2.4 Schering Bridge	18
2.5 Differential detector.....	19
2.6 Differential bridge.....	19
2.7 Pulse detector for PD energy measurement.....	22
2.8 Block diagram of single - channel analyzer (differential mode).....	23
2.9 ADC Ramp and pulse train	24
3.1 Block diagram of PD detection system	28
3.2 PD detection network.....	29
3.3 AC frequency response of PD detection network.....	31
3.4 Response of the high pass RC network.....	33
3.5 Response of the PSF to an exponential pulse across C_t	37
3.6 Response of the modified PSF to an exponential pulse across C_t	37
3.7 PD detection circuit with modified output impedance.....	38
3.8 Calculated AC frequency response of modified PD detection network.....	39
3.9 Experimental AC frequency response of modified PD detection network.....	40

Figure	Page
3.10 100 MHz Buffer amplifier	42
3.11 PD data acquisition and analysis system	43
3.12 A/D transfer function.....	44
3.13 Sampling time.....	46
3.14 Bi - slope triggering mode.....	60
3.15 Charge injection to sample capacitor.....	64
3.16 High voltage calibration mode	65
3.17 Calibration pulse e_c	68
3.18 Response of the PD detection network to a calibration pulse.....	68
3.19 Calibration of the test circuit	69
3.20 Voltage pulse used for calibration.....	70
4.1 Print-out of test 1 results	74
4.2 Pulse used in test 2.....	76
4.3 Typical partial discharge.....	79
4.4 Test results of specimen #8.....	81

CHAPTER 1

INTRODUCTION

1.1. Background

Partial discharges, basically electric discharges that do not produce a complete bridge between electrodes [1], cause progressive deterioration of an insulating material and may lead ultimately to insulator failure.

The terms corona and partial discharges have been often used in the literature to describe the same discharge phenomena [2]. In recent years, the term corona has been reserved for visible phenomena, that may occur on a high voltage transmission line [3], or around electrodes at low pressure conditions [4].

For phenomena that are not visible, because they are internal to a material or device, the term partial discharge is preferred. In the remaining chapters of this thesis, these phenomena will be referred as partial discharges or as PD.

Gas-filled voids or cavities within solid dielectrics are among the most common sources of partial discharges [5]. These cavities may be produced as a consequence of process control errors during the production of almost any type of solid dielectric or liquid-impregnated solid dielectric. Air leaking into the mold during curing may form a void, or insufficient pressure on the liquid epoxy during curing may permit a gaseous cavity to develop due to the vapor pressure of an epoxy component. In addition, foreign particles such as dirt, paper, textile fibers, etc., in the dielectric may lead to void formation.

The permittivity of the medium in a cavity is frequently lower than that of a solid insulation, which causes the field intensity in the cavity to be

higher than in the dielectric. Accordingly, under normal working stress of the insulation the voltage across the cavity may exceed the breakdown value and may initiate breakdown in the void.

The significance of partial discharges on the life of insulation has long been recognized. Every discharge event degrades the material due to the energy impact of high energy electrons or accelerated ions, which causes chemical transformations of many types.

The detection of partial discharges is based on energy exchanges which take place during the discharge. These exchanges are manifested as a) electrical impulse events; b) dielectric losses; c) electromagnetic radiation (light); d) sound; e) increased gas pressure; f) heat and g) chemical reactions. Discharge detection and measurement techniques may be based on the observation of any of the above parameters [6].

Several measuring systems and techniques have been devised over the years for partial discharge detection. These techniques encompass from the simplest and oldest "hissing test", where noise produced by discharges was used as an indication of their presence in the device under test, as well as modern digital instrumentation.

Basically, PD measuring systems can be classified as non-electrical or electrical, depending on which physical parameter associated with the discharges is measured.

Non-electrical systems measure energy exchange in the form of chemical transformation, gas pressure, heat, sound and light, the last two being of more practical importance [1]. There are two disadvantages associated with the use of non-electrical systems:

- Although they can detect the presence of internal discharges and their location in a dielectric sample, the discharge magnitude cannot be directly obtained.
- The testing environment plays an important role in the detection sensitivity, as in the case of sound detectors testing samples in noisy environments, where background noise drastically decreases the detection sensitivity.

The most frequently used and the most successful PD detection methods are electrical. These methods aim to separate the impulse currents linked with partial discharges from any other phenomena. The impulse current is then used to analyze the PD activity in the device under test.

Kreuger [1], identifies four steps that are needed for a complete correlation of partial discharges with their degrading effect on insulating materials: detection, measurement, location and evaluation.

Detection refers only to the certainty that discharges are present in the sample under test. Once a discharge pulse has been detected, its magnitude must be determined in the measurement stage. A physical quantity (or figure of merit) which is both relevant to the harmfulness of the discharges and can be measured with a discharge-detection method must be chosen. For some apparatus under test, like power transformers and high voltage cables, it is important to locate the precise source of partial discharges. This is not the case when testing small devices like capacitors with capacitances of the order of microfarads, for which the sensing of partial discharges is more important than pinpointing the PD site [7]. The last step, evaluation, allows an estimation of the type of danger that the detected discharges represent to the

insulation being tested, and the information thus obtained is used to predict the useful life of the sample under specific operating conditions.

This thesis is principally concerned with PD detection and analysis systems capable of detecting, measuring, displaying and performing an evaluation of the discharge activity of a device or material under test. Such systems are often referred to as "PD diagnostic systems"[8]. The information obtained is then used to get a better understanding of the degrading mechanisms of PD's.

Two commercially available PD diagnostic systems are most commonly used:

- PD energy measuring systems using a digital correlator [9, 10]
- Pulse height analyzers [8, 11]

1.2. Problem

Current research and development efforts to improve the ability of the electrical insulation systems to withstand energy discharges are heavily dependent on partial discharge diagnostic systems that can provide accurate and meaningful test data.

The primary purposes of PD analysis in research and development are basically to:

- Provide an empirical basis to correlate the PD behavior exhibited by different types of dielectric materials under different test conditions.
- Gain a better understanding of the physical mechanisms related to PD activity.

There are several experimental findings that support the need for fast and detailed analysis of partial discharges:

- Dielectrics under high stress conditions deteriorate due to the effect of microdischarges that take place in gas-filled voids or cavities within them [12].
- This deterioration increases with the number of discharges and is consequently proportional to the frequency of the applied voltage. The useful life of a dielectric is typically inversely proportional to frequency [12].
- The number of discharges also increases with increasing electrical stress in the dielectric. Moreover, the mechanism of deterioration is affected by electrical stress [13].

From these findings, it is clear that PD measurement systems able to produce individual pulse resolution from high frequency bursts will provide valuable data to characterize partial discharges.

There is also a tendency in the design of modern electrical and electronic systems to further stress dielectric materials:

- In aerospace applications, weight and physical size of electrical equipment can be reduced by an increase in operating voltages and frequencies [4]. Consequently, more stringent testing for PD is necessary in order to assure high levels of reliability.
- Electronic devices like capacitors have to withstand large and fast switching pulses associated with thyristors and power transistors in modern power electronics applications [8].

Unfortunately, conventional analog PD detection and analysis systems are not capable of performing high speed measurements because of their relatively narrow detection bandwidth (~ 10 KHz to several hundred KHz)

[8]. They have long time constants and in essence integrate the detected signals; individual pulses contribute only to an average value [14].

The development of digital instrumentation has made an important impact in the development of PD diagnostic systems. In modern equipment, two techniques are currently used: Pulse height analysis using a Multichannel analyzer (MCA), and PD energy measurement using a digital correlator. Although these systems are far faster than conventional analog PD detection systems, some drawbacks are associated with their performance:

- The processing time for each acquired pulse is made up of two components: the time required to "shape" a PD pulse by increasing its rise time before it is processed, in order to comply with the input signal requirement of the instrument, and the inherent time required for the instrument to process each pulse. The total time is in the order of 10 μ sec for the Multichannel analyzer [15], and 140 μ sec for the digital correlator [16].
- The data obtained from each pulse is used to perform a very specific type of analysis. Once a pulse has been processed no further inferences can be made about its waveshape.

There is then a need for a real time computer-based data acquisition system able to perform PD analysis according to the following characteristics:

- Broadband detection systems with capability of individual pulse resolution without the need of a shaping stage.
- Capability to produce valuable analysis from the individual pulse data, making it a very flexible system able to produce not only statistical information related to charge content but also to changes in repetition rate and waveshape characteristics.

- Automatic operation, so it can monitor life tests for long time frames without human intervention.
- Ease of operation, preferably menu-driven operation, so no complicated adjustments will be needed before each data acquisition.
- General purpose instrument that can be used to test different materials or devices under different test conditions.

1.3. Purpose

The purpose of this thesis is to design and build a computer-based PD diagnostic system having a sampling capability of 200 megasamples per second and being able to operate in either a manual or automatic mode.

This project has been sponsored by the National Aeronautics and Space Administration, NASA, as a research project to build a fast PD diagnostic system to be used in testing materials and devices for future applications at power frequencies of 20KHz. At this point in the project, the system has been fully tested at 60Hz and the preliminary testing at high frequency voltages has been started. The block diagram of the proposed system is shown in Fig. 1.1.

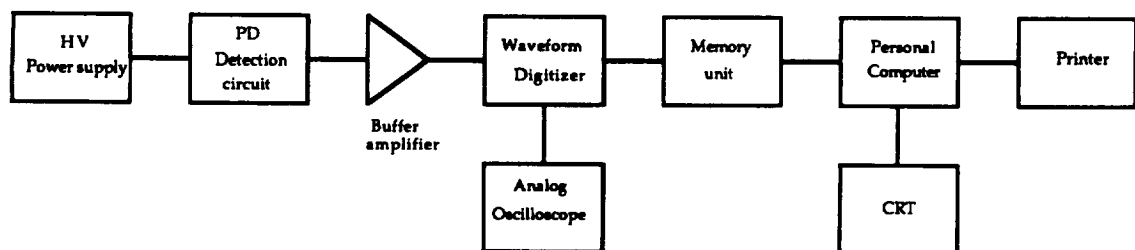


Fig. 1.1. Block diagram of PD Detection System

This experimental system consists of 3 main parts:

- a) High voltage source;

b) PD detection network;

c) Data acquisition and analysis system.

The high voltage source is a 100KV, 5KVA PD free transformer, having a regulatable output voltage from 1KV to 100KV. The PD detection system is a RC network performing as a "straight PD detector" [1], where the discharges of interest are separated from the power frequency voltage and the discharge pulse voltage across a detection impedance is measured. The data acquisition and analysis system consists of a 200 MHz digitizer in combination with a 4 Megaword memory unit connected to an IBM compatible computer through a General Purpose Interface Bus (GPIB). Using dedicated software, the computer controls the complete operation of the data acquisition system, by setting the instrument's front panel acquisition controls, analyzing the digitized data from each pulse and producing statistical analyses of the charge content of each partial discharge.

CHAPTER 2

LITERATURE REVIEW

2.1. Introduction

Commercially available instrumentation for the measurement of partial discharges has been developed primarily for two applications: manufacturing quality assurance and service life assessment.

The first one is the largest application for PD measuring equipment, although a few systems, like the one reported by Boggs [17], have been developed for PD measurements on installed systems.

Quality assurance covers PD testing during design and manufacturing of insulated equipment, cables, devices and all electrical systems whose reliability depends, to a great extent, on their capability to operate satisfactorily for several years under high field conditions.

PD testing is specified for a very wide range of high field systems, and high field systems nowadays include even many different types of low voltage applications, such as integrated circuits which operate at very low voltages across such thin dielectrics that the phenomena of charge injection and degradation, usually associated only with highly stressed high voltage dielectrics, can occur [18]. This means that high electrical stress does not necessarily require high voltage.

The variety of instrumentation and measurement techniques for partial discharges is as extensive as the different applications for the materials and systems to be tested. In some cases of corona in air, the only concern is radio interference and appreciable levels of PD are tolerable. In other cases, such as solid dielectric materials used at high stress ($> 2.5 \text{ KV}_{\text{rms}}/\text{mm}$), no PD

should be detectable at the highest test voltage and the greatest available PD detection sensitivity.

In general, and through experience, manufacturers and users now have a clear understanding of the manufacturing process limitations. Because of this, it is possible to determine the maximum PD level that can be tolerated and the service life expected for a particular class of apparatus.

An electrical PD measuring system consists basically of two components: a PD detection circuit and a pulse processing unit. Both have to operate together as a coordinated system that maximizes the measuring sensitivity required for the specific type of apparatus or material under test.

Over the years, several combinations of detection circuits and pulse processing units have been used, and because of the large variety of such systems, it is rather difficult to make a general classification. Kreuger [19] has classified the PD measuring systems based on the number of inputs to the detection circuit. Steiner [14] uses a different approach, making a classification on the grounds of not only the number of inputs but also on bandwidth of the detector and method of display information. A literature survey was conducted in order to determine, as completely as possible, all of the different commercially available PD measuring systems in use today. In order to cover this subject in an organized way, we will review detection networks first and then the complete PD measuring systems.

2.2. Detection networks.

Four basic network topologies are most commonly used for PD detection:

- RLC networks
- Discriminating circuits

- Loss detectors
- Differential or balanced detectors

These detection circuits can be classified according to two characteristics: number of inputs and bandwidth.

A brief description of each one of these basic topologies will be provided in this chapter. In addition, references to publications where more detailed information about their performance can be found will be included.

Depending on the number of inputs, a detection circuit can be classified as: a) single input (or "straight detection method" [1]), where a voltage or current signal (and any interference) is measured at some point of the test object, and b) multiple input, used to reduce the effect of interference. The most common multiple input system uses two detection impedances. When these impedances are similar, the circuit is called balanced. Black [21] presents a very interesting report on PD pulse detection using balanced networks in noisy environments.

With respect to bandwidth, PD detection circuits can be classified as narrowband or broadband. The distinction between them is based upon the ability of the circuit to resolve individual pulses. If the bandwidth of the detector is sufficiently wide to resolve individual pulses, then the detector is considered to be broadband, otherwise it is narrowband.

In general, commercial PD detection systems are bandpass in nature: the signals of interest are small pulses superimposed on large, power frequency voltages, and successful detection of the pulses requires separating them from the power frequency voltages. Narrowband measuring systems have long time constants and in essence integrate the detected signals; individual pulses contribute only to an average value [20].

2.2.1. RLC networks.

The most common circuit used for partial discharge detection is based on a RLC network. In Fig.2.1, a schematic diagram of a typical RLC PD detection network is shown. This circuit is implemented basically using a high voltage coupling capacitor terminated in a measuring impedance.

This combination, also known as the pulse detection network or as the power separation filter (PSF) [8], has a high pass filtering effect similar to that of a single pole RC differentiating network. Stray inductances and nonideal components influence the response of these networks, but their primary behavior can be modeled as the second order response of an RLC network.

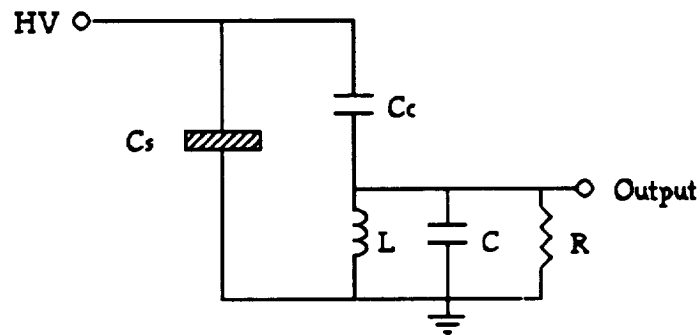


Fig. 2.1. RLC network

It is important to recognize that the coupling capacitor C_c must be PD free up to the maximum test voltage used for a particular specimen.

The PSF is a broadband single input detector, used by most PD detection systems, as reported in [8, 9, 22]. In chapter 3, a detailed description of the operation of this circuit is provided.

2.2.2. Discriminating circuits.

A PD discriminating circuit may be constructed by connecting two RC detection circuits in parallel, as shown in Fig.2.2. This topology and an associated discriminator have been reported in [21] to reduce considerably the effect of interference on measurements of partial discharges in a noisy environment. This circuit can be classified as a multiple input, broadband detector.

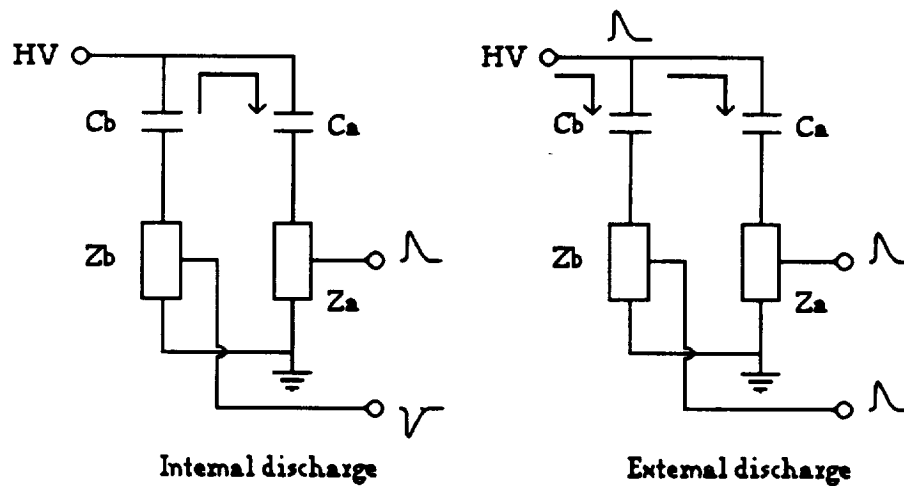


Fig. 2.2. Discriminating circuit

The operation of the circuit is based on the following concept: when an interfering pulse couples into the measuring system from an external source, the current pulses induced in the detection impedances generate voltage drops with the same polarity. Conversely, if a partial discharge pulse occurs in either capacitor, C_a or C_b , the voltages from each of the two detection impedances will have opposite polarity. A double channel instrument will then use the polarity of the pulses to discriminate against external noise. This technique is also referred as a common mode rejection method.

This detector improves the sensitivity of partial discharge measurements in situations where one or more of the following problems are present:

- The HV transformer is not discharge-free at the operating voltage.
- Corona is present in the external circuit
- The supply line voltage contains pulse interference.

One of the advantages of this system is that the coupling capacitor does not have to be discharge-free, and may even be replaced by a second test component. This is possible when the polarity of the pulses is also compared to the instantaneous applied voltage. Based on the fact that partial discharge pulses will have polarities that depend on the instantaneous polarity of the test voltage, the discriminating instrument can determine whether the PD pulse occurred across Ca or Cb. If a partial discharge occurs in Ca during the positive half cycle of the test voltage, a positive voltage is then expected across the detection impedance connected to Ca.

One of the disadvantages of this system is that strong interference may cause the the system to block almost completely the processing of signals, and become almost "blind". This occurs because whenever a noise pulse is present, the discriminating instrument cannot respond to any incomming pulses for a time typically of the order of 10 μ sec. Consequently, continuous interference can cause the system to become saturated.

To solve this problem, a subtraction technique is used to reduce the continuous interference before the signals are processed by the discriminator.

2.2.3. Loss Detectors.

Loss detectors are commonly used to measure the dielectric strength of insulating materials. Their use is based on the concept that an electrically

stressed dielectric will exhibit losses due to its inherent conductivity. If partial discharges are present, they will cause additional changes in the original values (i.e., with no discharges) of capacitance and dissipation factor of the specimen under test.

A real dielectric can be represented by the configuration in Fig.2.3a, i.e., as a parallel combination of a resistance R and capacitance C . Fig.2.3b is the vector diagram of the electrical response of the circuit, where angle θ (or phase angle) represents the angle by which current leads voltage. If the conductance of the sample (G), is zero as with an ideal capacitor, θ is equal to 90° ; and if $C = 0$, as for a perfect resistor, then θ will be equal to 0 . From Fig.2.3b follows that

$$\tan \delta = \frac{1}{\omega RC} \quad (2.1)$$

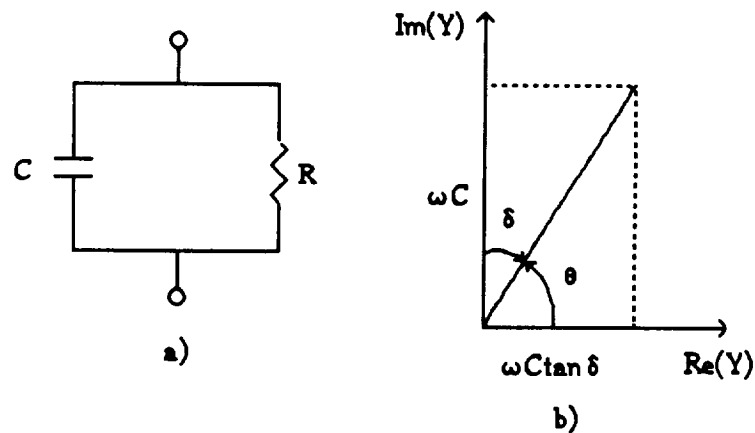


Fig. 2.3. Real dielectric representation

Conduction through a resistor, unlike conduction through a perfect capacitor, must always cause joule heating. By observation of Fig.2.3b, $\cos \theta$

can be related to a measure of the resistive component of the impedance and hence the rate of heat generation or electrical power absorption. For materials with very little conduction, $\cos\theta$ can be considered equal to $\tan\delta$, which is commonly referred as the dissipation factor or "loss tangent" of the dielectric.

As reported by Dakin [23], internal discharges in a dielectric will cause the capacitance and dissipation factor of the sample to change from their initial values in the absence of internal discharges. This change in the value of $\tan\delta$ is commonly used in quality assurance to evaluate the dielectric strength on stator coils and windings of high voltage rotating machines. The method is known as "power factor tip up". The validity of the change of $\tan\delta$, $\Delta\tan\delta$, as a measure of PD activity is extensively discussed by Kelen in [24].

$\tan\delta$ has a particular advantage as a measure of the quality of a specimen of insulation: it is dimensionless, and because of this fact, direct comparisons can consequently be made on similar materials having widely different geometries [25].

The most common loss detector in use today is the Schering bridge. Fig. 2.4 shows a schematic representation of the basic configuration of this bridge.

The specimen dielectric is placed in one of the arms of the Schering bridge. The value of $\Delta\tan\delta$ can be obtained by balancing the bridge once internal discharges are present in the specimen. PD's in the specimen dielectric (represented by Z_x) will cause an unbalance in the bridge that can be compensated by an adjustment in the values of R_1 and C_1 . The relationship between $\tan\delta$ and the values of impedance Z_1 will be found for the balance conditions:

$$Z_x = Z_2 \cdot Z_3 \cdot Y_1 \quad (2.2)$$

By expanding this expression and equating the real and imaginary terms,

$$R_x - \frac{j}{\omega C_x} = R_2 \left(\frac{-j}{\omega C_3} \right) \left(\frac{1}{R_1} + j\omega C_1 \right) \quad (2.3)$$

$$R_x = \frac{R_2 C_1}{C_3} \quad (2.4)$$

and

$$C_x = \frac{C_3 R_1}{R_2} \quad (2.5)$$

By representing the dielectric sample as a parallel combination of a capacitor C in parallel with a resistor R, as explained above, and using (2.4) and (2.5), the following relationship can be obtained [26]:

$$\tan \delta = \frac{1}{\omega R C} = \omega R_x C_x = \omega R_1 C_1 \quad (2.6)$$

Consequently, by balancing the bridge through the variable capacitance C1, a reading on the change of $\tan \delta$ can be obtained, and thus be directly related to the appearance of partial discharges. In other words, at a voltage below V_i (PD inception voltage), the measured value of loss tangent represents the dielectric loss in the solid insulation; above V_i an additional contribution to the measured value of loss tangent is made by the energy loss due to partial discharges.

The basic topology of the Schering bridge of Fig.2.4 has been modified over the years in order to improve sensitivity and eliminate stray capacitances. A complete discussion of the different loss detectors in use is given by Baker in [25].

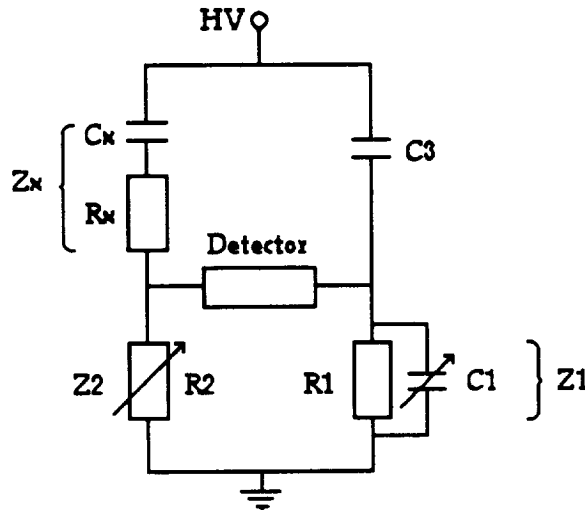


Fig. 2.4. Schering Bridge

2.2.4. Differential detectors.

Differential detectors are commonly used when individual pulse resolution is required when testing for PD's in noisy environments.

The test system is configured as a bridge detector, and a basic topology for this circuit is depicted in Fig.2.5. The device under test is connected in the specimen arm of the bridge. If the standard capacitor with impedance Z_s is identical to the specimen, the bridge will be balanced. Otherwise, the variable impedances Z_1 and Z_2 must be adjusted to reach balance.

When the bridge is balanced, any interference coupled into the system becomes a common mode signal which induces equal voltages at the detector inputs. The signal is sensed as a differential voltage across the detection transformer, so any common mode signals cancel.

A variation of this topology, known as a differential bridge, is shown in Fig.2.6. In this circuit, balance is achieved by changing only the transformer turns ratio, making this detector very easy to balance.

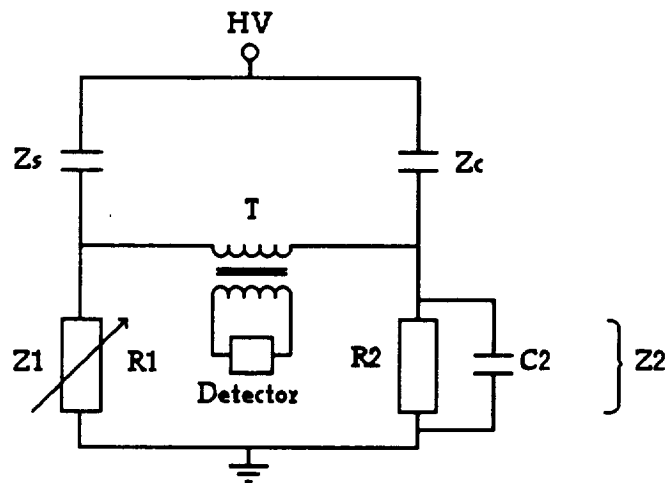


Fig. 2.5. Differential detector

The disadvantage with this network is that large currents in the specimen will also flow through the detection transformer, and construction of a precision wideband transformer of the quality required in a bridge detector with adequate current capacity is difficult.

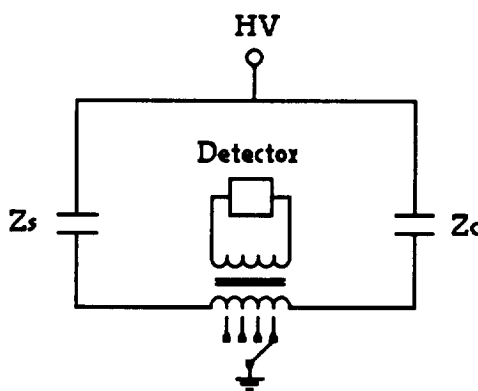


Fig. 2.6. Differential bridge

2.3. Pulse processing instruments.

Pulse processing instruments can be classified according to the way in which the pulse information is processed and displayed. Three basic types can be identified:

- Direct display
- Meter display
- Computer-based systems

2.3.1. Direct display.

A direct display instrument operates like an oscilloscope; the detected pulse is displayed directly on a CRT. One of the most common direct displays used for PD detection has an elliptical time base mode, in which the partial discharge pulses are displayed around the perimeter of an ellipse. The ellipse is displayed in such a way that top and bottom coincide with the positive and negative peaks of the high voltage sine wave and the ends coincide with the zero crossings. The discharge patterns displayed in this way give a good indication of the type and source of the partial discharges. Standard discharge patterns can be found in the instruction manuals for commercially available instruments using this type of display [27].

2.3.2. Meter display.

This type of display is associated with integrated measurements and is implemented as a digital panel meter or as an analog meter movement.

The information provided is a quantity related to partial discharge activity, the most common being the PD charge content in Coulombs.

Instruments like the HAEFELY PD detector [27] use a meter display to complement simultaneously its elliptical time base display.

2.3.3. Computer based systems.

The development of digital instrumentation has made possible significant advances in the knowledge of the degradation mechanisms of partial discharges; the PD pulses are not only "seen" on the screen of the

oscilloscope but can also be detected individually and their waveform characteristics can be stored in digital form to be used later for a great variety of analysis.

The most common commercially available computer-based instruments under this classification are digital correlators and pulse height analyzers.

2.4. Computer-based PD diagnostic systems.

2.4.1. Digital correlator.

Some investigators [9, 10] have reported the use of a digital correlator to measure energy instead of charge as a figure of merit for PD. This method is based on the fact that energy is an inherent property of the discharge, and that an energy supply is essential to sustain a degradation process.

The measurement of energy is carried out by an evaluation of the following expression:

$$E_t = \sum_{i=1}^N U_i Q_i \quad (2.7)$$

where E_t is the energy supplied by the source over the time period t during which N discharges have been produced, Q_i and U_i being respectively the apparent charge of discharge i and instantaneous value of the applied voltage at the moment of the discharge.

This summation of products is performed by using the analysis characteristics of a digital correlator. This instrument is basically a signal analyzer capable of computing and displaying 100 points correlating functions. A complete description of the digital correlator, which is beyond

the scope of this report, can be found in [16]. The important feature of the digital correlator is its ability to perform a mathematical operation with the following characteristics:

$$R_{xy}(\tau) = \frac{1}{N} \sum_{k=1}^N x(k \Delta t - \tau) \cdot y(k \Delta t) \quad (2.8)$$

where x and y are the two waveforms to be correlated, N is the number of times the evaluation will take place (or number of samples taken), τ is the delay time used for correlation purposes and Δt the sampling rate. The instrument is able to perform the above calculation for 100 different values of τ , but for the specific application of the PD energy measurement, only the case for which τ is equal to zero is of importance. Waveforms x and y will be identified with U_i and Q_i , respectively.

In Fig. 2.7, a topology for pulse detection and simultaneous measurement of the instantaneous value of the applied voltage is provided. As can be observed, the pulse detection arm of the circuit is basically a power separation filter, as described earlier in this chapter.

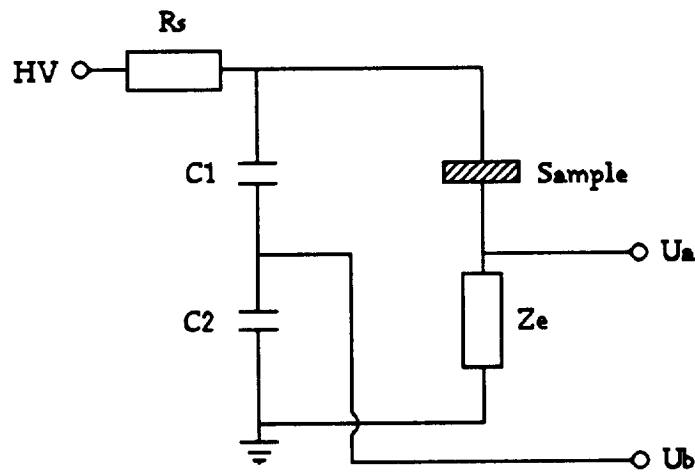


Fig. 2.7. Pulse detector for PD energy measurement

Although the concept presents very interesting possibilities for the measurement of PD energy instead of charge, the instrument requires a minimum of 140 μsec to evaluate each pulse. Consequently, it is unable to process pulses that occur with a frequency greater than 7 KHz.

2.4.2. Pulse height analyzers.

In conventional Partial discharge measuring systems, as described in [8, 11, 28], pulse height analysis is extensively used.

This type of analysis is performed by commercially available instruments known as single channel analyzers (SCA) or multichannel analyzers (MCA).

These instruments classify a pulse by its height within certain preselected ranges, and the output of the analysis is a count of the number of pulses that occurred within these ranges or intervals. Internally, the equipment converts the height of the pulse (in Volts) to a charge level (in Coulombs). If the analysis is made by sampling one channel at a time, the apparatus is called SCA. Thus, the SCA is capable of recording only those pulses falling within a single channel or section of an energy spectrum; all other pulses are rejected. In Fig. 2.8 a block diagram of a typical SCA is shown.

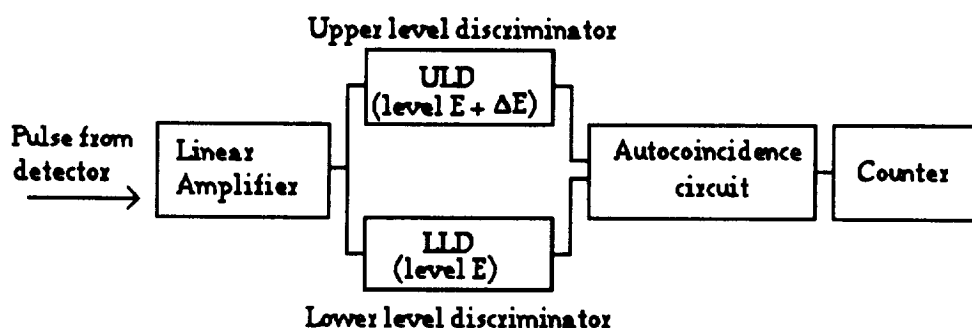


Fig. 2.8. Block diagram of single-channel analyzer (differential mode)

A significant limitation of the SCA, is its inability to perform a complete analysis of an energy spectrum in a reasonably short time, because in order to cover n channels, one must examine sequentially point by point n individual channels, and this process takes a long time. Consequently, this equipment is not useful for complete PD measurements over long periods of time.

In most practical PD detection systems, a MCA is used to perform pulse height analysis. MCAs help to avoid the limitations of the SCAs by making possible a faster scan analysis of an energy spectrum.

The basic principle of operation of the MCA involves an analog to digital converter (ADC) as developed by Wilkinson, Hutchinson and Scarot [15, 28]. The process can be summarized as follows: first, a small capacitor is charged up to the peak of the incoming pulse; it is then discharged at constant current. While the discharge is in progress, clock pulses from a stable oscillator are counted by a scaler; the number of clock pulses counted is proportional to the time the capacitor takes to discharge, and hence to the original height of the pulse. This process is depicted in Fig. 2.9 [15].

The ADC converts the pulse height to a number proportional to the energy of the event. This number identifies a dedicated memory location, and one count is added to the contents of that memory location.

After data have been collected for some period of time, the memory contains a set of numbers that correspond to the number of pulses in each energy level bin.

As expressed in [28], the MCAs are capable of recording most of the pulses associated with an energy spectrum. The only pulses not recorded are those that occur while the analyzer is busy handling a previously acquired

pulse. The time required for the MCA to process one single pulse is in the order of $10\mu\text{sec}$.

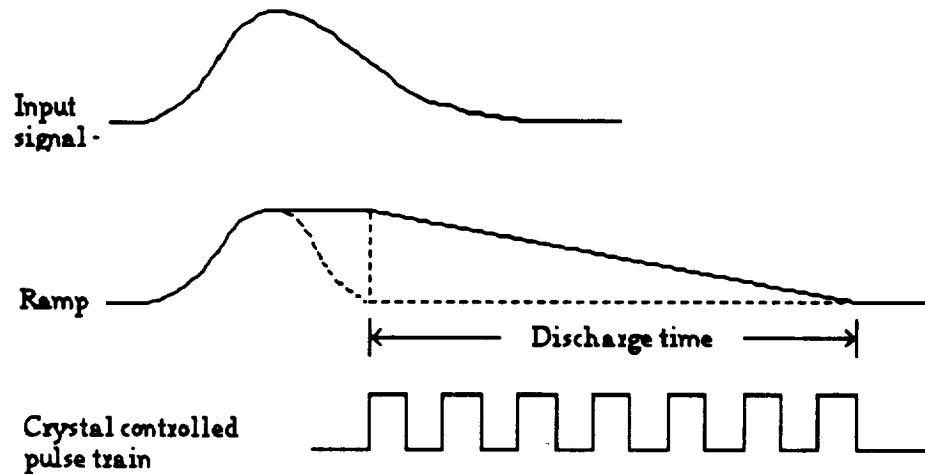


Fig. 2.9. ADC Ramp and pulse train

The above description and the technical data of commercially available MCAs lead to three important aspects of MCA performance for our investigation: first, pulses having fast risetimes ($< 1\ \mu\text{sec}$ as specified for the CANBERRA Series 35 PLUS Multichannel Analyzer [15]) must be "shaped" prior to being input to the instrument in order to increase the rise time of those pulses. As described in [8], a pulse-shaping amplifier can be used to increase the magnitude and duration of the incoming pulses.

Second, the MCA is not able to process all incoming pulses from a high frequency burst, because of the time required to evaluate each one of them. And finally, once the information about the pulse height of a single pulse has been obtained, no information is available about the shape of the pulse, so no further conclusions about changes in the characteristics of the waveshapes under different test conditions can be drawn.

2.5. Conclusions from the literature review:

1. A dielectric under high stress conditions deteriorates due to the effect of microdischarges that take place in gas-filled voids or cavities contained within it.
2. These cavities are produced in most cases due to process control errors during the production of almost any type of solid dielectric or liquid-impregnated solid dielectric.
3. Partial discharges produce reduction in the useful life of a dielectric material. Consequently, a need to detect, measure and analyze the nature of those discharges has arisen.
4. Several measuring systems and techniques have been devised for partial discharge detection. Detection schemes which are most sensitive tend to be application specific, while those which are of general applicability tend to sacrifice some sensitivity.
5. Basically, PD detection systems can be classified as electrical and non-electrical. Electrical systems are more commonly used.
6. The bandwidth of the detection system limits the quality of the information that can be obtained. For research and development purposes, systems capable of single pulse resolution are preferred.
7. Two commercially available instruments most commonly used for PD analysis are Multichannel analyzers and Digital correlators.
8. These instruments present processing time constraints due to the "dead" time associated with the processing of an individual pulse.
9. There is a need for fast computer-based PD diagnostic systems in order to study PD degrading mechanisms in highly stressed dielectrics exposed to high voltage and high frequency AC power sources.

CHAPTER 3

DESCRIPTION OF THE SYSTEM

3.1. Introduction

Most of the PD diagnostic systems in use today are based on the concept of pulse height analysis, although some investigators have reported the use of a digital correlator to perform PD energy measurements [9, 10]. Two important disadvantages limit the quantity and quality of the data obtained by using those instruments: a) the time required to process each pulse could easily prevent a large number of pulses from being analyzed for high frequency burst sources, and b) the data of each waveform cannot be stored for further experimental work to correlate pulse characteristics with time, cavity size and shape, dielectric material and frequency of the AC source.

In this thesis, a new PD measurement and analysis system is described. Its overall characteristics and flexibility of operation make it a suitable option for long duration test experiments, needed to increase the understanding of the effect of PD's in the aging process of dielectrics.

3.2. General description

This new experimental system consists of 3 main parts:

- a) High voltage source;
- b) PD detection network;
- c) Data acquisition and analysis system.

A block diagram of this system is shown in Fig. 3.1. The high voltage source and detection network were located inside ASU's high voltage laboratory, a completely shielded room acting as a Faraday cage [29].

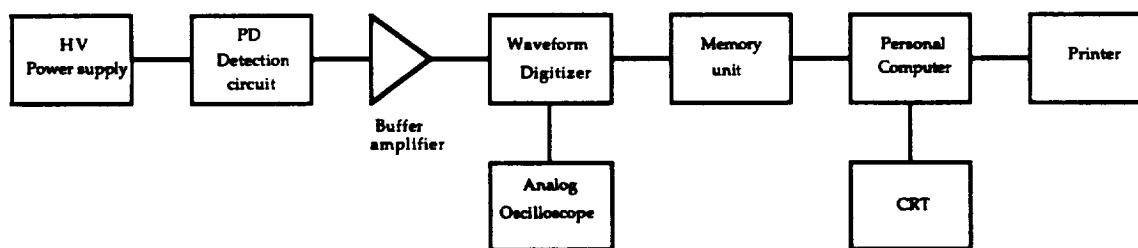


Fig. 3.1. Block diagram of PD Detection System

3.2.1. High voltage source

The HV supply for the PD measurement system includes a HAEFELY 100KV, 5KVA PD free HV transformer, having a regulatable output voltage from 1KV to 100KV. The high voltage transformer was connected to the PD detection system by means of a 100 Ω , 175W wirewound ceramic resistor, which is used to limit the secondary current if insulation breakdown occurs.

3.2.2. PD detection network

The circuit used for the detection of the partial discharge pulses can be classified as a broadband, single input detection circuit [14]. A schematic of the circuit used is shown in Fig. 3.2, and its physical realization contains the following elements: a 150pf, 30KV vacuum capacitor used as a HV coupling capacitor; a RC network of one 150 Ω , 1/2W carbon resistor in parallel with a 220pf, 60V mica capacitor, used to compensate for stray inductances in the detection circuit [8]; a 50 Ω , 1/2W carbon resistor used as a detection impedance. This is the basic configuration of the PD detection circuit used. A modification to the output impedance R_d was made during the experimentation in order to improve the output pulse characteristics. This modification will be presented later in this section.

The network of Fig.3.2 is also known as a Power Separation Filter (PSF) [8, 14], because of its high pass filtering capability that is similar to that of a

single pole RC differentiating network. Stray inductances and nonideal components influence the response of these networks; so in the physical realization of the circuit the following considerations were observed in order to reduce the effect of stray elements:

- The leads of all elements were kept as short as possible.
- Carbon resistors were used instead of wirewound ones, because of their inherently smaller inductance.
- Elements C1, R1, Rd, D1 and D2 were all contained within a small metallic box which structure was connected to the system ground.

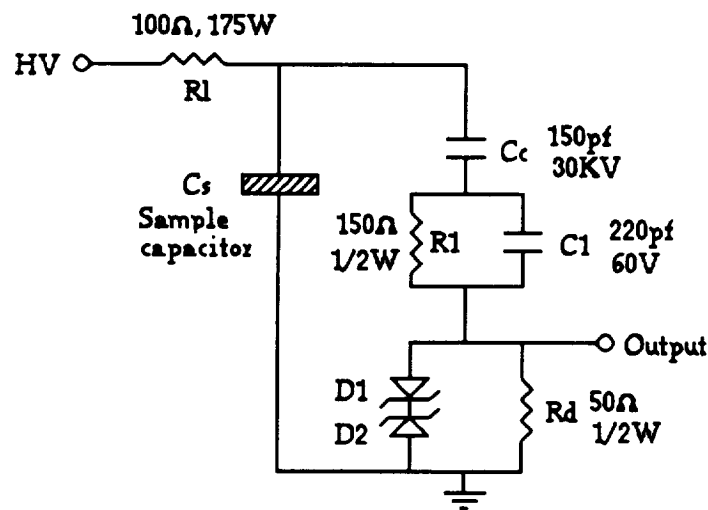


Fig. 3.2. PD detection network

In order to protect the measuring instrument from high amplitude transient pulses, that can be generated at the breakdown of a sample or by the switching of the HV supply, two zener diodes D1 and D2 with minimum breakdown voltage of 25V were connected as shown in Fig. 3.2.

The AC frequency response of this circuit was calculated with PSPICE 4.04, a circuit simulator, by sweeping an AC input signal from 1KHz to 1GHz.

The results of this simulation are presented in Fig.3.3, and the listing of the PSPICE file used to generate this response can be found in Appendix A.1.

The cut-off frequency (lower 3dB frequency) of the circuit can be found from [28]:

$$f = \frac{1}{2 \pi R_d C_c} = 21.22 \text{ MHz} \quad (3.1)$$

where $C_c = 150\text{pF}$ and $R_d = 50\Omega$. Elements C1 and R1 do not affect appreciably this value, as can be observed in Fig. 3.3. These results indicate that the 60 Hz power frequency voltage is expected to be attenuated by:

$$A = -20 \log \frac{f_1}{f_2} = -110.97 \text{ dB} \quad (3.2)$$

were $f_1 = 21.22 \text{ MHz}$ and $f_2 = 60 \text{ Hz}$. Experimentally, the attenuation observed was -109.03 dB , a value consistent with the theoretical results expected.

An analysis of the behavior of this circuit as a high-pass RC network to 4 different input signals at node 1 was prepared using the following functions: a) sine-wave; b) step-function (step-voltage); c) pulse input and d) exponential waveform.

3.2.2.1. Sine-wave function

If v_i is a sine-wave of frequency f applied across the combination in series of capacitor C_c and resistor R_d (the simplest representation of our power separation filter), the output v_o at R_d represented as a function of frequency is:

$$v_o = v_i / \left(1 + \left(f_1 / f \right)^2 \right)^{\frac{1}{2}} \quad (3.3)$$

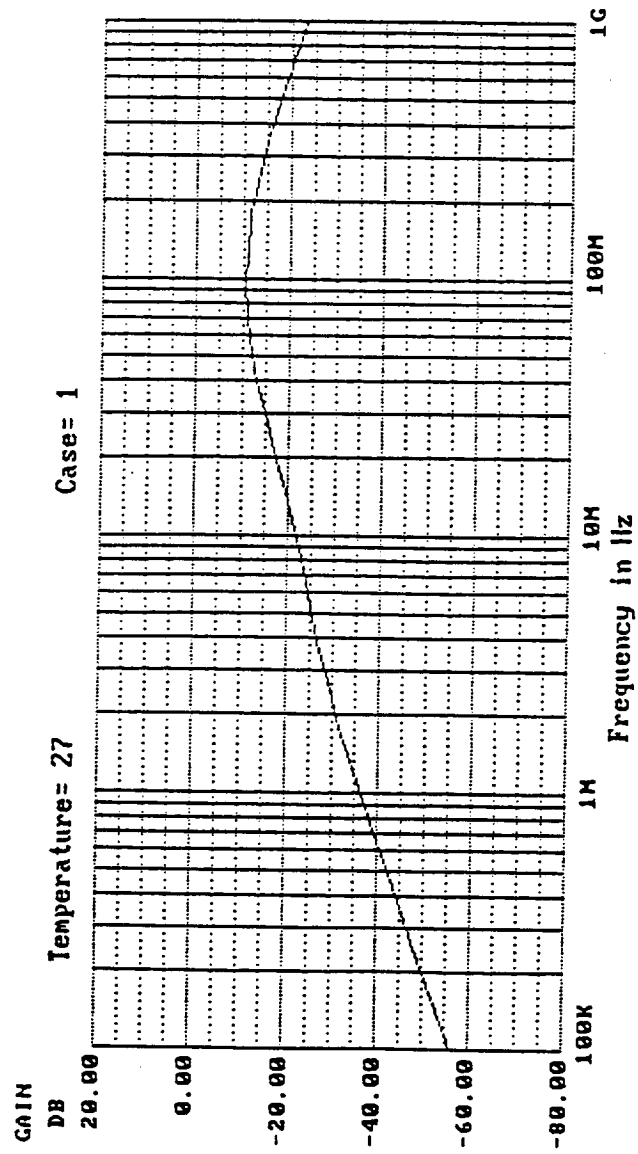


Fig. 3.3 AC frequency response of PD detection network

where the denominator $(1 + (f_1/f)^2)^{1/2}$ is the magnitude of gain of the network and f_1 is the lower 3-dB frequency equal to $1/2\pi R_d C_c$ as mentioned earlier. At the frequency f_1 the magnitude of the capacitive reactance is equal to the resistance R_d and the gain is 0.707. A Bode plot representing the response of the circuit is presented in Fig. 3.3.

3.2.2.2. Step function

The response of this RC network to a step-voltage input is exponential, with a time constant $\tau = R_d C_c$. The output voltage has the form:

$$v_0 = v_f + (v_i - v_f) e^{-\frac{t}{\tau}} \quad (3.4)$$

where v_f and v_i are the final and initial output voltages, respectively of the step-voltage function. For $t > 0$, the input is a constant, and since C_c blocks the dc component of the input, the final output voltage is zero, or $v_f = 0$. Then equation 3.4 becomes:

$$v_0 = v_i e^{-\frac{t}{RC}} \quad (3.5)$$

3.2.2.3. Pulse input

If the pulse in Fig. 3.4a is applied to the RC network, the response for times that are less than the pulse duration t_p is the same as that for the step voltage input. At the end of the pulse, the input falls abruptly by the amount V , and, since the voltage at C_c cannot change instantaneously, the output must also drop by V . Thus immediately after $t = t_p$ (or at $t = t_p +$), $v_0 = v_p - V$; v_0 becomes negative and then decays exponentially to zero. For $t > t_p$, v_0 is given by:

$$v_0 = V \left(e^{-\frac{tp}{RC}} - 1 \right) e^{-\frac{(t-tp)}{RC}} \quad (3.6)$$

If $R_d C_c \gg t_p$, there is only a slight tilt to the output pulse and the undershoot is very small, as shown in Fig. 3.4b. If $R_d C_c \ll t_p$, the output consists of a positive spike of amplitude v at the beginning of the pulse and a negative spike of the same size at the end of the pulse, as shown in Fig. 3.4d.

3.2.2.4. Exponential input

In any RC network, $v_i = q/C + v_o$, where q is the capacitor charge. Differentiating this equation gives:

$$\frac{dv_i}{dt} = \frac{i}{C_c} + \frac{dv_o}{dt} \quad \text{or} \quad \frac{dv_i}{dt} = \frac{v_0}{R_d C_c} + \frac{dv_o}{dt} \quad (3.7)$$

Suppose the input of the network is an exponential waveform given by:

$$v_i = v(1 - e^{-\frac{t}{\tau}}) \quad (3.8)$$

where τ is the time constant of the input wave. Then equation 3.7 becomes:

$$\frac{v}{\tau} e^{-\frac{t}{\tau}} = \frac{v_0}{R_d C_c} + \frac{dv_o}{dt} \quad (3.9)$$

Defining n and x by $n = R_d C_c / \tau$ and $x = t / \tau$, the solution of equation 3.9 [35], subject to the condition that the capacitor voltage is initially zero, is given by

$$v_o = \frac{n v}{n - 1} (e^{-\frac{x}{n}} - e^{-x}) \quad (3.10)$$

if $n \neq 1$ and by

$$v_o = v x e^{-x} \quad (3.11)$$

if $n = 1$.

Near $t = 0$, the output follows the input. Also, the smaller $R_d C_c$ is, the smaller the output peak at R_d .

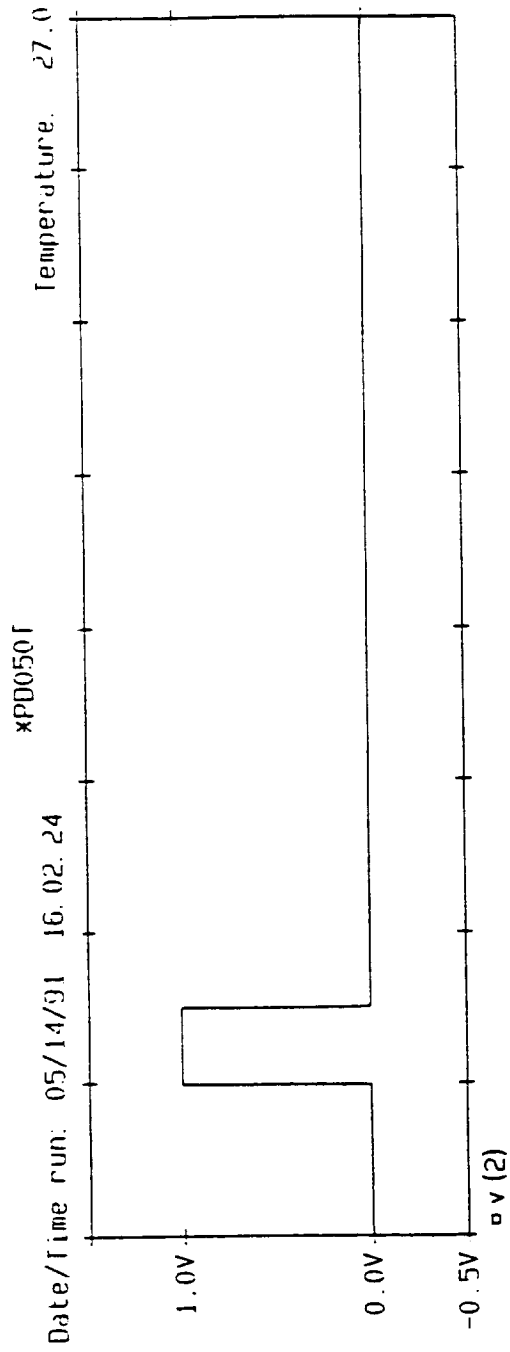


Fig. 3.4 a Input pulse

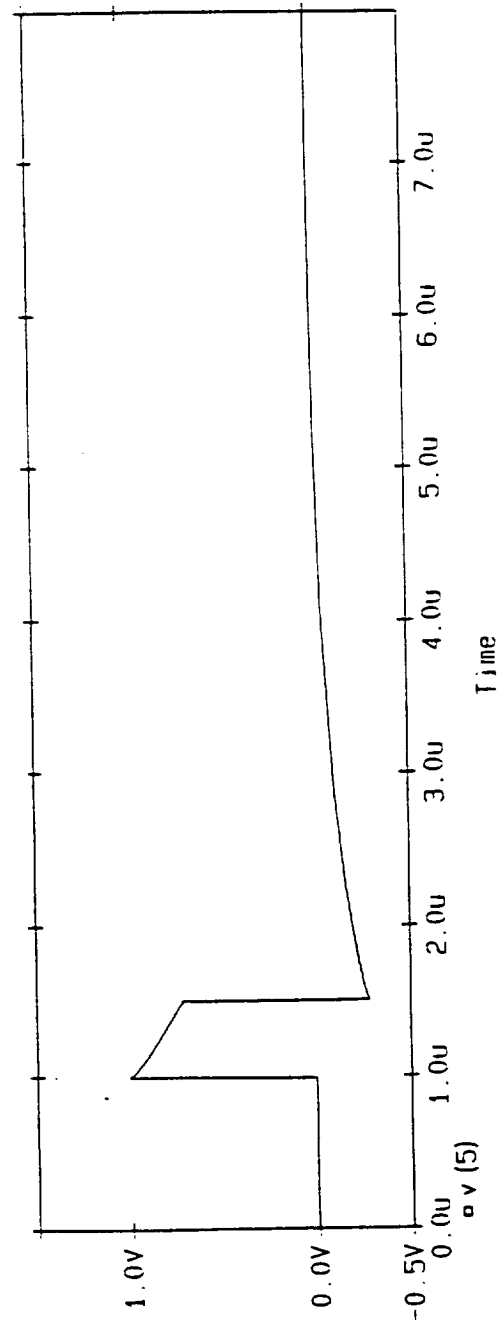


Fig. 3.4 b Response of the high pass RC network if $RC \gg t_p$

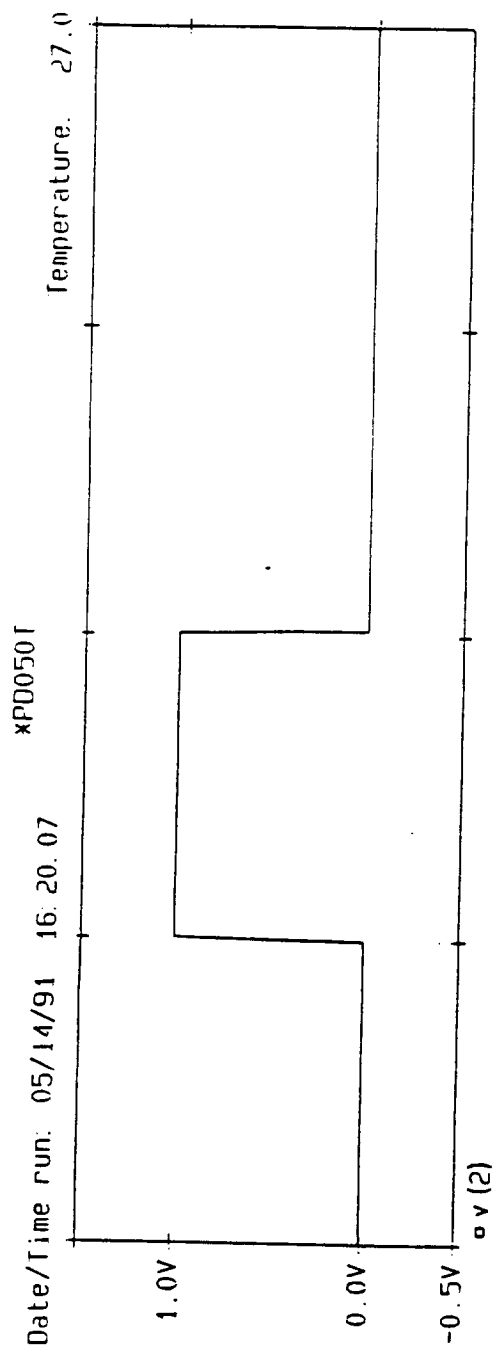


Fig. 3.4 c Input pulse

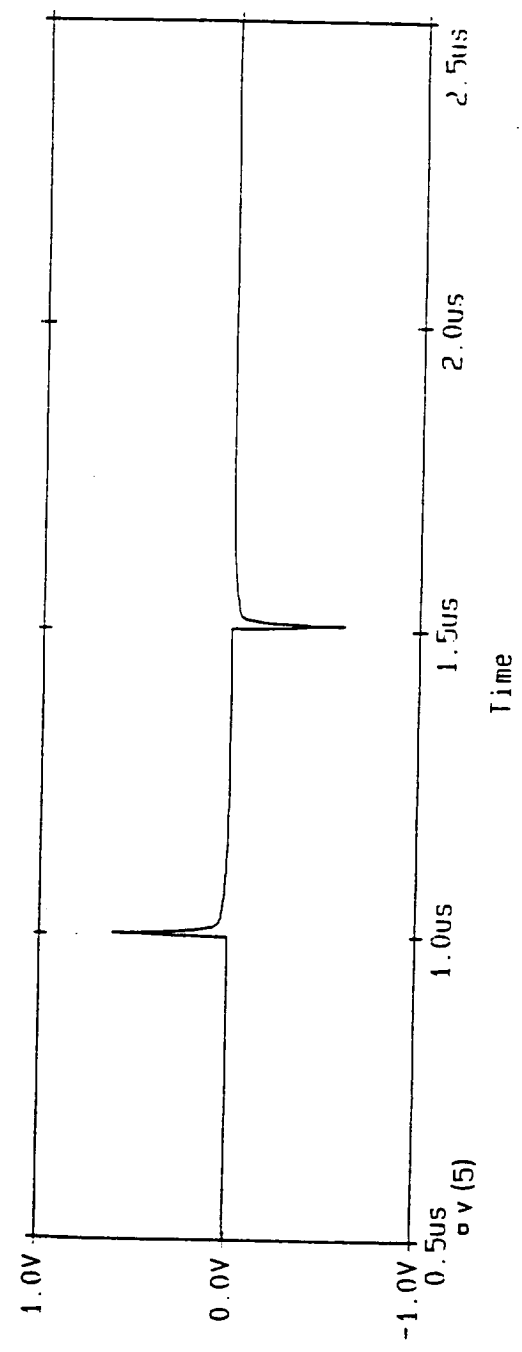


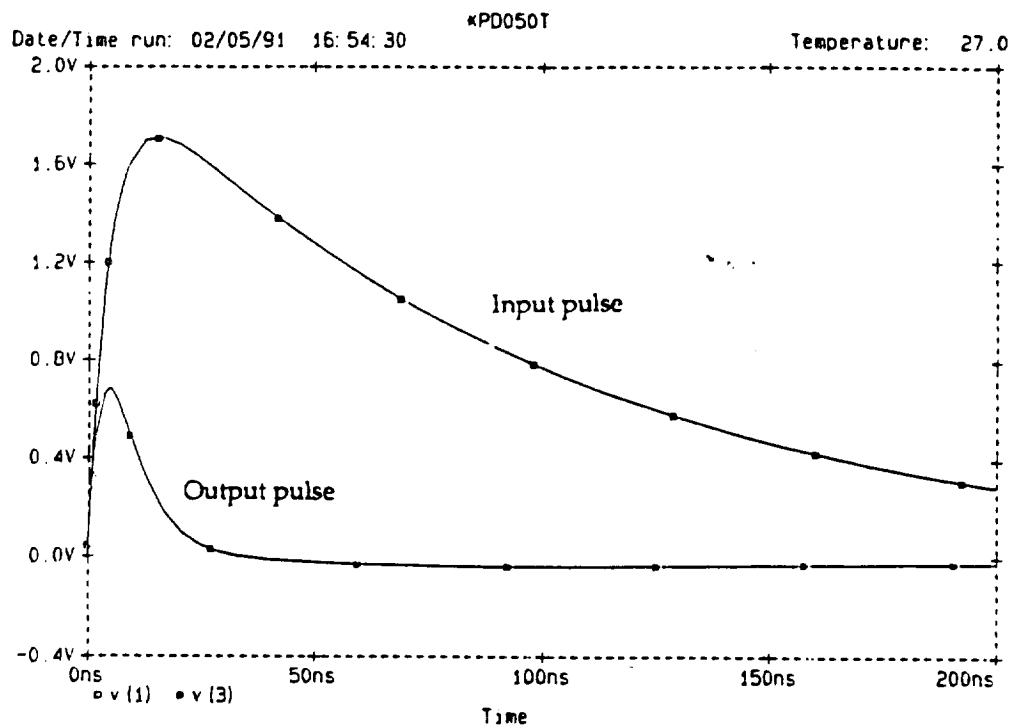
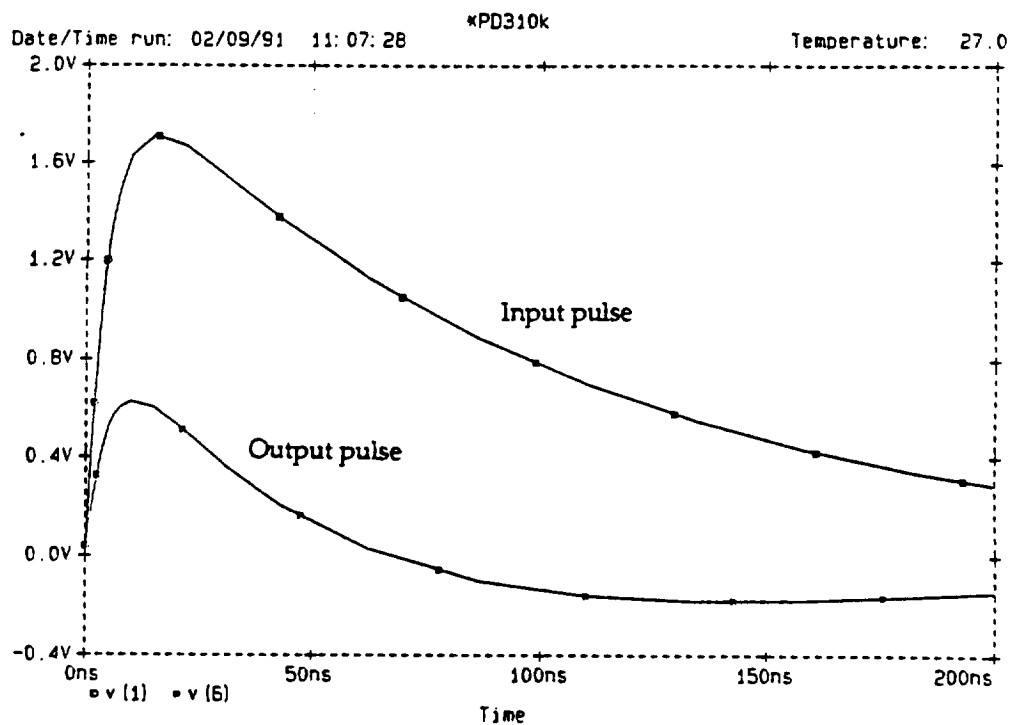
Fig. 3.4 d Response of the high pass RC network if $RC \ll t_p$

If the value of the coupling capacitor is fixed, along with all the parameters in the circuit including stray capacitances, the resistor R_d will determine the response of the circuit. Unfortunately, increasing the value of R_d from 50Ω produces a mismatch of impedances with the measuring instrument. An effort was conducted to improve the response of the circuit by modifying the detection impedance without producing ringing of the signal. In order to simulate testing conditions, exponential waveforms were used as input signals to the network.

It is reasonable to assume that typical partial discharges will have characteristics close to an exponential waveform, with fast risetimes and long decay times [12]. Consequently, an input signal having a risetime in the order of 5 nsecs. and decay time of 100 nsecs was applied to the detection system across the terminals of the sample capacitor to sense the expected response of the circuit to PD's. This response was obtained using PSPICE 4.04, and the input and output waveform are shown in Fig. 3.5. The characteristics of the exponential waveform used in the simulation were determined from the characteristics of actual PD's observed and recorded in previous tests.

With a change in the output impedance in the PD detection circuit, the characteristics of the original pulse were recovered with satisfactory result. When using an input signal with the same characteristics as in the case presented in Fig. 3.5, the output signal obtained with this new arrangement had characteristics closer to the original waveform, as can be observed in Fig. 3.6.

The major change made in the circuit was the substitution of a cascaded set of three high-pass RC filters, as depicted in Fig. 3.7, for the 50Ω detection

Fig. 3.5 Response of the PSF to an exponential pulse across C_t Fig. 3.6 Response of the modified PSF to an exponential pulse across C_t

resistor. Resistors R_{d1} , R_{d2} , R_{d3} and R_{d4} are $10\text{K}\Omega$, $1/2\text{W}$, carbon resistances and C_d , C_{d2} and C_{d3} are 10 pF , 60V , mica capacitors.

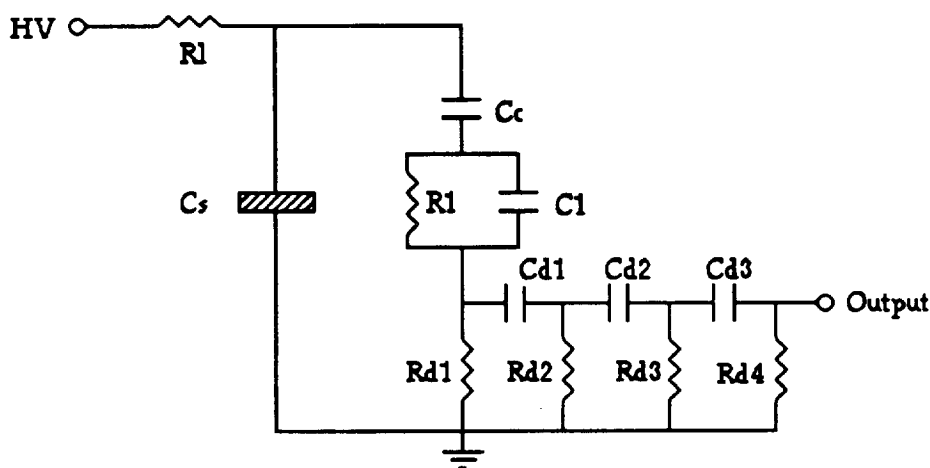


Fig. 3.7. PD detection circuit with modified output impedance

As with the circuit in Fig. 3.2, simulation was performed using PSPICE 4.04 to observe AC and transient responses of this new arrangement. The frequency response is shown in Fig. 3.8 and, as can be observed, a level of attenuation of -9 dB was calculated in the frequency range from 3MHz to 200 MHz . These calculated results were correlated with experimental data, by using a TEKTRONIX type 190B constant amplitude signal generator, with variable output frequency in the range of 100kHz to 50MHz .

The experimental frequency response, presented in Fig. 3.9, has characteristics close to the calculated results, with a maximum difference of -4dB at 2 MHz .

This level of attenuation was only possible when using low capacitance cables (LEADER LP160X), having a total capacitance of 24.4 pF as measured with a PHILLIPS model PM6303 RCL meter. When using standard RG-58

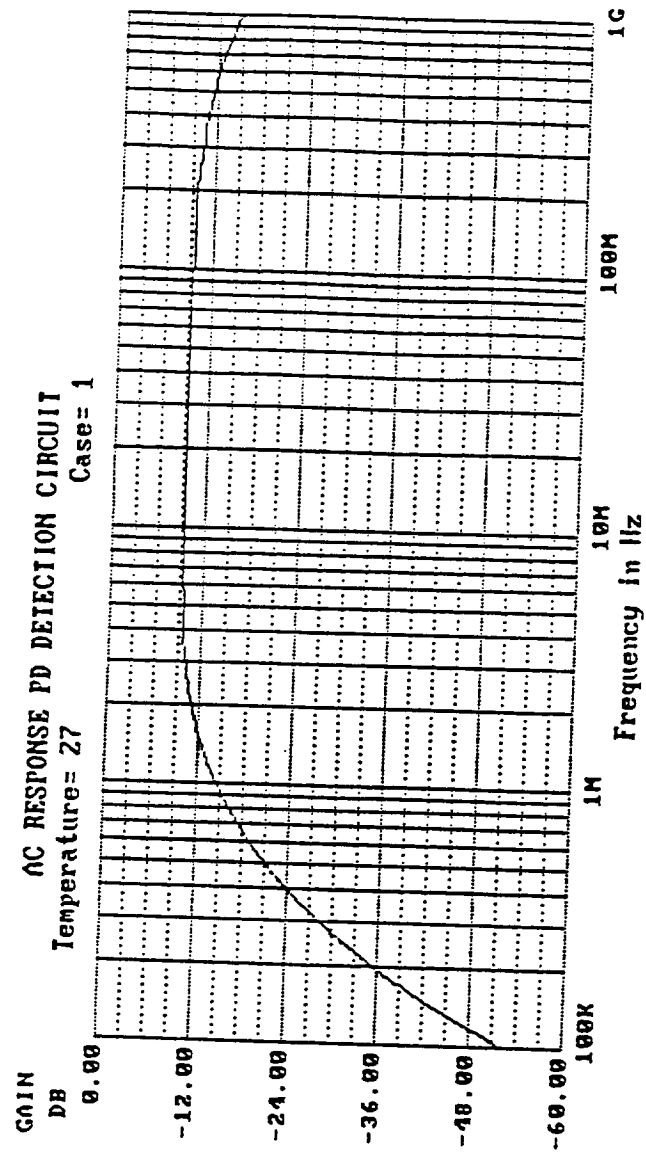


Fig. 3.8 Calculated AC frequency response of modified PD detection network

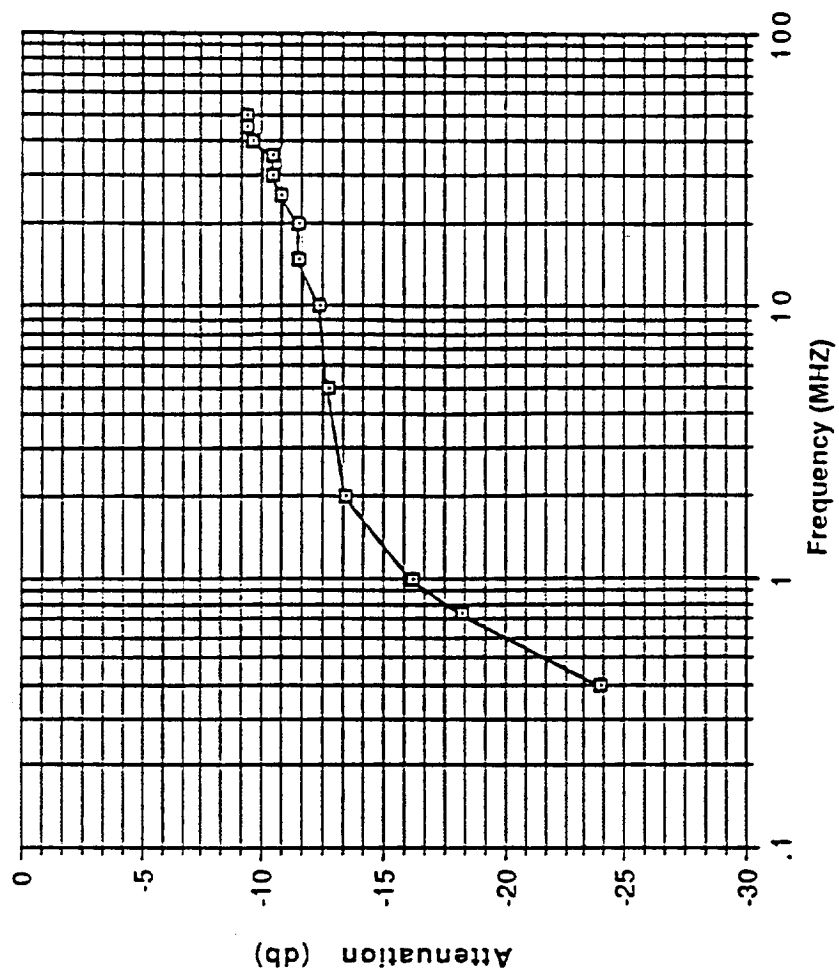


Fig. 3.9 Experimental AC frequency response of modified PD detection network

coaxial cable, a capacitance of 28.5 pF/ft is expected, and 5 feet of this cable produced -16dB loss experimentally in the same range of frequencies and under the same test conditions.

One of the problems found in the new arrangement was the distortion of the output signal due to ringing. This effect was produced by signal reflection due to the mismatch of impedances between the detection circuit and the input impedance of the instrument.

With a low input impedance (50Ω) at the instrument, the ringing effect disappeared, but this arrangement was undesirable, because the high output impedance ($10K\Omega$) of our detection circuit had no effect on the output signal characteristics, because it was shunted by the instrument's low impedance.

An impedance matcher presenting a high input and low output impedance was connected between the PD detection circuit and the instruments. This circuit permits a pulse to be sensed across the PD detection circuit output impedance, and the input of the instrument can be set to 50Ω , to match the coaxial cable impedance.

This circuit has the required characteristics needed for our specific applications: high input and low output impedances, fast slew rate and broad bandwidth. The key element in this circuit is a National Semiconductor device LH0063. A diagram of this amplifier circuit is given in Fig. 3.10.

This amplifier has a gain of 1 for a bandwidth of 100 MHz, and produces excellent results for matching of impedances between the detection resistance and the instrument's low input impedance (50Ω). The only limitation found when using the LH0063 is its inherent dc offset of 5mV. This component can be compensated at the data acquisition stage, as will be explained in the next chapter. New amplifiers with virtually no output dc

components are now been investigated, like the AVANTEK GPD 462, with a frequency bandwidth of 200 MHz, a constant gain of 9dB and with the advantage that only one dc source is required to power it.

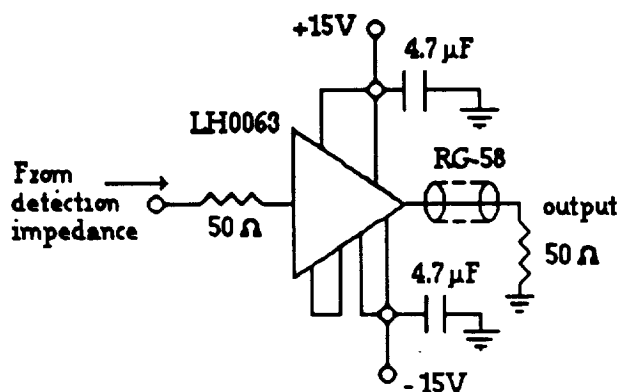


Fig. 3.10. 100MHz Buffer amplifier

RC detection topologies are most commonly used to resolve individual PD pulses when testing in controlled experimental environments, that is, assuming that the following conditions are satisfied in the testing facilities:

- The HV transformer is discharge free at the testing voltage;
- Corona is not present in the external circuit;
- The supply line voltage does not contain high frequency interference;
- The coupling capacitor is PD free at the testing voltage.

To make sure these assumptions were valid in our laboratory, the system was tested at high voltage with the sample dielectric C_s removed.

The applied voltage was increased gradually and a TEKTRONIX 2430A digital oscilloscope was used to monitor discharge activity across the detection impedance R_d . No pulses were detected up to 8.5KV rms; beyond that voltage, small pulses with an amplitude of less than 2mV were observed.

3.2.3. Data acquisition and analysis system

The heart of the proposed PD diagnostic system is the data acquisition and analysis stage. This subsystem consists of the following elements:

- a) Real time waveform digitizer;
- b) Fast Data Cache;
- c) General Purpose Interface Bus (GPIB);
- d) IBM compatible computer;
- e) Software (ASUPD v.1.7).

A schematic of the data acquisition system is shown in Fig. 3.11.

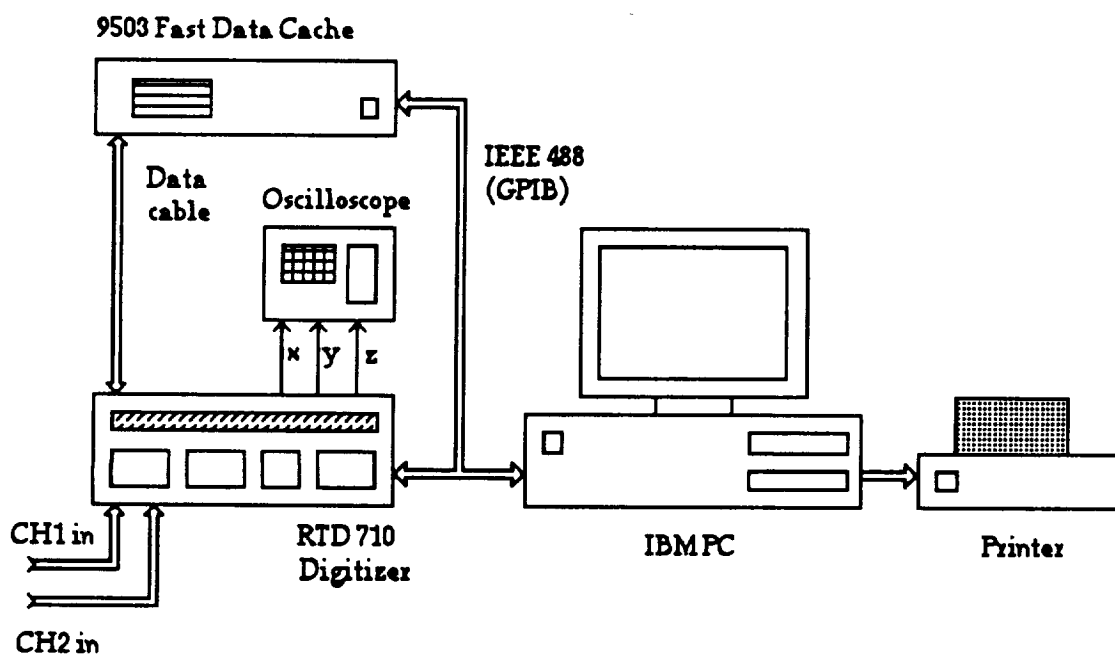


Fig. 3.11. PD data acquisition and analysis system

Before we attempt a description of the different parts of the system, it is important to mention some theoretical aspects of analog-to-digital (A/D) converters, to provide a better understanding of the terminology involved in data acquisition systems.

3.3. Data acquisition systems theory

The following is a basic introduction of data acquisition theory. The author found extensive information in [28, 30, 31]. The areas to be covered in this section are quantizing, sampling and coding theory.

3.3.1. Quantizing theory

Analog to digital conversion is basically a two-step process: quantizing and coding. Quantizing is the process of transforming a continuous analog signal into a set of discrete output states. Coding is the process of assigning a digital code word to each of the discrete output states. For example, in a 3-bit A/D converter, 8 different output states are possible, as a sequence of binary numbers from 000 to 111. As can be observed in Fig. 3.12, if the analog input signal varies from 0V to +10.0V, then +1.25V will be the discrete voltage assigned to the binary number 001, +2.50V assigned to 010 and so on.

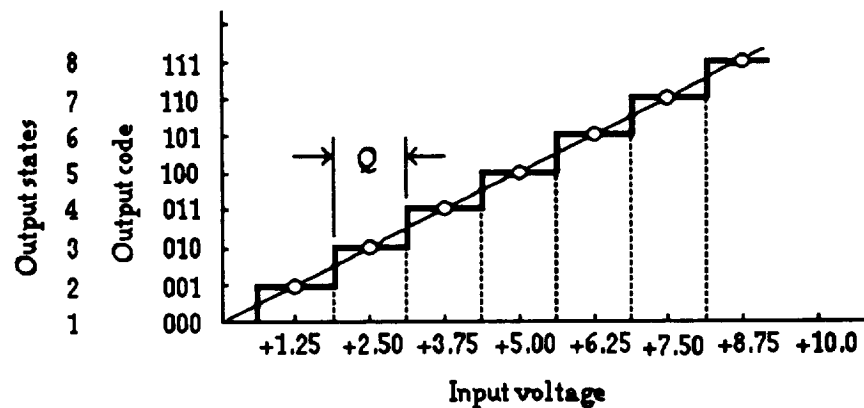


Fig. 3.12. A/D transfer function

There are several important points concerning the transfer function of Fig. 3.12. First, the resolution of the A/D converter is defined as the number of output states expressed in bits; in the case of our example, the converter has a 3-bit resolution. The number of output states for an A/D converter is 2^n ,

where n is the number of bits. Consequently, an 8-bit converter has 256 output states, and a 10-bit converter has 1024 output states. As shown in Fig. 3.12, there are $2^n - 1$ analog decision points in the transfer function. These points are for example voltages +0.625 and +1.875, where +1.25 is the center point of the output code word 001. The analog decision point voltages are precisely halfway between the code word center points.

At any part of the input range of the A/D converter, there is a small range of analog values within which the same output code word is produced. This range is the voltage difference between two adjacent decision points and can be found from the following expression:

$$Q = \frac{FSR}{2^n} \quad (3.12)$$

where FSR stands for "Full Scale Range", or 10.0V in our example, and n is the number of bits of resolution of the A/D converter. Evaluating (3.12) with the values given in our example, Q is equal to 1.25V. In this expression, Q represents the smallest analog difference which can be resolved, or distinguished by the converter. If the number of resolution bits is increased, this error is much smaller. For example, if $n=10$, the error in our case will be reduced to 9.76mV.

3.3.2. Sampling theory

An A/D converter requires a small, but significant, amount of time to perform the quantizing and coding operations. The time required to make the conversion depends on several factors: the converter resolution, the conversion technique, and the speed of the components employed in the converter. The conversion speed required for a particular application

depends on the time variation of the signal to be converted and on the accuracy desired.

Conversion time, also known as aperture time or sampling time [30, 31], refers to the time uncertainty (or time window) in making a measurement and results in an amplitude uncertainty (or error) in the measurement if the signal is changing during this time.

As shown in Fig.3.13, the input signal to the A/D converter changes by a value of ΔV during the sampling time t_s in which the conversion is performed.

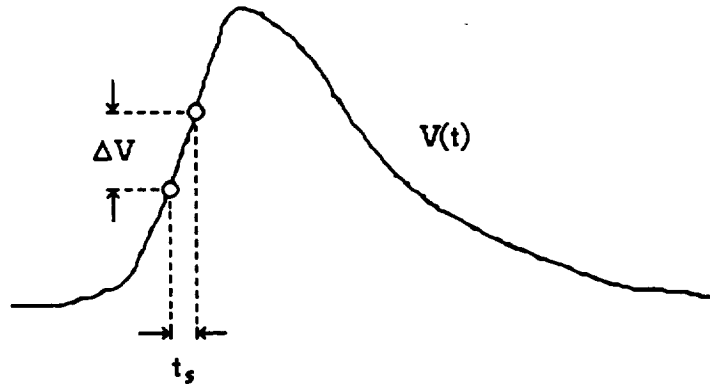


Fig. 3.13. Sampling time

This difference can be considered an amplitude error or a time error; the two are related as follows:

$$\Delta V = t_s \frac{dV(t)}{dt} \quad (3.13)$$

where $dV(t)/dt$ is the rate of change with time of the input signal. For the specific case of a sinusoidal input signal, for example, the maximum rate of change occurs at the zero crossing of the waveform, and the amplitude error is:

$$\Delta V = t_s \frac{d}{dt} (A \sin \omega t)_{t=0} = t_s A \omega \quad (3.14)$$

The resultant error, expressed as a fraction of the peak to peak full scale value is:

$$\epsilon = \frac{\Delta V}{2A} = \pi f t_s \quad (3.15)$$

This result indicates that the sampling time required to digitize a 1 KHz signal to a 10 bits resolution is:

$$t_s = \frac{\epsilon}{\pi f} = 320 \text{ nsecs.} \quad (3.16)$$

where ϵ is one part in 2^{10} or approximately 0.001.

3.3.3. Coding theory

A/D converters interface with digital systems by means of an appropriate digital code. While there are many possible codes to select, a few standard ones are almost exclusively used with data converters. The most popular code is "natural binary", or straight binary, which is used in its fractional form to represent a number:

$$N = a_1 2^{-1} + a_2 2^{-2} + a_3 2^{-3} + \dots + a_n 2^{-n} \quad (3.17)$$

where each coefficient "a" assumes a value of zero or one, and the resulting value N has a fractional value between zero and one. As an example, consider a binary fraction that would be normally written as 0.110101. With data converter codes the decimal point is omitted and the code word is written 110101. This code word represents a fraction of the full scale value of the converter and has no other numerical significance. The binary code word 110101 therefore represents the fraction 0.82775, where $n = 6$:

1	x	2^{-1}	=	0.5
1	x	2^{-2}	=	0.25
0	x	2^{-3}	=	0.0
1	x	2^{-4}	=	0.0625
0	x	2^{-5}	=	0.0
1	x	2^{-6}	=	<u>0.01525</u>
				0.82775

or 82.77% of full scale of the converter. If full scale is +10V, then the code word represents +8.2775V. The natural binary code belongs to a class of codes known as positive weighted codes, since each coefficient has a specific positive weight. The leftmost bit has the most weight, 0.5 of full scale, and is called the most significant bit, or MSB. The rightmost bit has the least weight, 2^{-n} of full scale, and is therefore called the least significant bit or LSB. The bits in a code word are numbered from left to right from 1 to n.

The LSB has the same analog equivalent value as the quantizer error Q, that is:

$$\text{LSB} = \frac{\text{FSR}}{2^n} \quad (3.18)$$

An important point to notice is that the maximum value of the digital code, namely all 1's, does not correspond with analog full scale but rather with one LSB less than full scale, or $\text{FSR} \times (1 - 2^{-n})$. Consequently, a 10-bit resolution converter with a 0 to +10V analog range has a maximum possible code of 11 1111 1111, and this number represent a maximum analog value of $+10 (1 - 2^{-10}) = +9.99023\text{V}$. In other words, the maximum analog value of the converter, corresponding to all 1's in the code, never quite reaches the point defined as analog full scale.

3.4. Operation of the PD acquisition and analysis system proposed

A PD pulse across the detection impedance of the RC network will be present at one of the input channels of the waveform digitizer. If this pulse reaches a predefined voltage level, a trigger pulse will be generated internally in the digitizer and a sampling and recording process will start.

The A/D stage produces a string of binary code values, or "record", that represents the original analog pulse voltage waveform. This string of binary code data is stored temporarily in memory. The number of elements in this array depends directly on the memory size assigned to it by the user, as it will be explained below in the description of the instruments.

Once all the data points of a memory record have been acquired, the digitizer will hold until a new trigger pulse is generated to start acquisition of another pulse. This process will repeat until all the predefined number of records have been acquired and stored.

When all the required number of pulses have been recorded, a data transfer between the memory unit and the PC will start, one PD pulse record at a time. The PC will analyze the data of the transferred string, and produce statistical information related to peak voltage value and charge content per pulse.

In the case of peak value of the pulse, the maximum binary value found in the array, either positive or negative, will be "scaled" to its analog equivalent voltage value. The total number of pulses acquired will be distributed according to their respective amplitudes. This is accomplished by setting the number of bin levels n to be used for comparison purposes and incrementing a count value assigned to each pair of bin levels according to the actual amplitude of the pulse being analyzed. For example, if the

amplitude of a pulse P1 is greater than the bin level L1 but smaller than the immediate superior bin level L2, where L1 and L2 are two consecutive bin levels, the count assigned to the pair L1-L2 will be increased in one unit, to indicate that the PD pulse acquired had an amplitude within L1 and L2.

For charge content of the pulse, the absolute value of the peak voltage will be multiplied by the calibration factor of the particular sample under test. The calibration process will be discussed later in this chapter. As in the case of the peak voltages, the number of bin levels n for charge comparisons is also provided. The charge content of the pulse under analysis is compared with successive bin levels, and a count is increased accordingly.

Once the analysis has been completed, a measurements file containing the count values of all the bin level pairs can be sent to a printer.

3.5. Description of the instruments

3.5.1. Real Time Waveform Digitizer

The waveform digitizer used was a fully programmable TEKTRONIX RTD 710 digitizer, whose electrical specifications are given in Table 3.1. More detailed technical information about this instrument can be found in [31, 32].

The RTD 710 acquires an incoming analog waveform through channels 1 and/or 2, producing a digitized stream of information that can be sent to an external memory unit for further analysis.

The sampling rate will determine how closely the digitized information will represent the original analog waveform. Depending on the particular application, different sampling rates can be selected. For this particular digitizer, a maximum sampling rate of 100 MHz (10nsecs) is possible in dual channel mode, or 200 MHz (5nsec) in single channel or "Channel 1 only" mode. An explanation for this difference is the following:

TABLE 3.1

TEKTRONIX RTD 710 Waveform Digitizer
Electrical Specifications

Input Channels:	2, single ended. Supports X10 and X100 encoded probes for high input voltage applications
Input Range:	± 100 mV to ± 50 V (200 mV to 100 V p-p) in 28 steps.
Analog Bandwidth:	DC to 100 MHz
AC - coupled lower -3dB point:	10 Hz or less
Input impedance:	$1\text{ M}\Omega \pm 2\%$; 24 pF
Internal clock frequency:	200 MHz $\pm 0.001\%$
Sample rate:	Single channel mode, 200MS/s; Dual channel mode, 100MS/s.

when the digitizer operates in dual channel mode, one sample acquired at channel 1 requires, as a minimum, a processing time of 5 nsecs. The sample to be acquired then at channel 2 will require another 5 nsecs, consequently, every sample at each channel takes a total of 10 nsecs.

The RTD 710 allocates a total of 32K 10 bit words of memory for each channel. This memory is quite flexible; it can be divided into smaller record lengths (1K, 2K, 4K, 8K or 16K).

The number of records available in dual channel mode can vary from one record (with 32K word length) to 32 records (with 1K length each). In our application we use the "Channel 1 only" mode, which allows the memory to have 64K words available and a maximum sampling rate of 200 MHz.

This digitizer has a total vertical resolution of 2^{10} (1024) points. The A/D scaling factor needed to convert digital to analog information is found by dividing the predefined voltage range of the input channel by the total resolution (1024):

$$SF = \frac{2V}{1024} \quad (3.19)$$

The RTD710 can be set for a particular application by selecting its acquisition parameters from the front panel or by programming them using a GPIB (General Purpose Interface Bus). For our application, an IBM personal computer was used to set up the digitizer.

The three major groups of parameters are:

- a) Trigger
- b) Recording mode
- c) Record length

3.5.1.1. Trigger characteristics

The RTD 710 has 3 trigger modes with which to begin the recording of a waveform:

- 1) Auto: The recording function free runs, recording the base line in the absence of a triggering signal.
- 2) Normal: Recording starts with the occurrence of a valid trigger signal. The digitizer waits for the trigger before storing waveform information.
- 3) Single: One record is made after the trigger event occurs. After the recording ends, the digitizer enters the Hold state.

This digitizer has many triggering capabilities, but for the present work only one was used, the bi-slope triggering mode. This capability combines the positive and negative slope trigger modes, in the sense that a trigger window can be created between two predefined levels, one sensing when a particular positive going pulse crosses the upper (or positive) trigger level and one sensing when a negative going pulse crosses the lower (or negative) trigger level. This function is very useful when the polarity of the pulses from a particular source is unknown.

3.5.1.2. Recording mode

Of the four different recording modes provided in this digitizer, the NORMAL mode was used for our work. In this mode, the digitizer acquires a full waveform and depending on the selected trigger mode, as explained above, the digitizer will stop the acquisition when a single record has been filled or when it is triggered to acquire new information.

3.5.1.3. Record length

As explained above, the built in memory of 32K 10 bit words per channel can be divided in smaller sections depending on the particular application. If the Channel 1 only mode is used, the memory available is 64K words, allowing up to 64 different records of 1K words each.

In order to perform analysis of the digitized information, the data for each waveform has to be sent to a computer unit. There, with the aid of suitable software, information about voltage or current peak levels, charge and repetition rate can be obtained. The RTD 710, working by itself, is able to send through the GPIB bus a maximum of 64 records once its internal memory has been filled. It will then wait until all the information has been processed by the computer before it starts again to acquire a new set of waveforms.

For accurate results in long duration tests, this limited memory is potentially a problem, because of the size of the sample to be used for statistical analysis. An external memory unit capable of storing data at the same speed the digitizer is producing it was needed.

3.5.2. Fast Data Cache

The number of pulses to be obtained in each set was greatly increased by the use of a TEKTRONIX 9503 Fast Data Cache (FDC), a memory unit that is responsible for storing digitized information up to 4 Mwords prior to sending data to the computer. In Table 3.2 the key electrical specifications of this apparatus are presented.

The FDC buffer memories provide significant record length augmentation for high speed, real time digitizers like the RTD 710.

TABLE 3.2

TEKTRONIX FDC 9503 Fast Data Cache
Electrical Specifications

Input Channels:	2 independent channels
Data inputs:	16 bits, clock, ground; selectable between ECL and TTL, in groups of 4 bits.
Memory size:	2Mwords/channel or 4Mwords total.
Recording rate:	100 Mwords/sec in Normal, Sequential and pretrigger modes. 200 Mwords/sec in Interleave mode (with RTD 710 in high speed mode).

This unit accepts up to 16 bit words plus clock, at up to 100 Megawords (samples) per second. Record lengths may range from 256 words to 2 Megawords per channel. The total memory of both channels can be combined into one large memory of 4 Megawords.

There are four recording modes available for the FDC 9503, Normal, Sequential, Pretrigger and Interleave. In all but the Interleave mode, recording speeds up to 100 Megasamples per second (10 nsecs per data point) are possible. In the Interleave mode, in conjunction with the RTD 710 in high speed mode, data can be recorded at a rate of 200 Megasamples per second (5nsecs per sample).

3.5.3. General Purpose Interface Bus (GPIB)

The General Purpose Interface Bus (GPIB) is essentially a cable having a total of twenty-four conductors, of which sixteen are devoted to signal transmission [33]. Signals on those conductors can be manipulated to transfer data in both directions between devices connected to the cable. Eight of the sixteen conductors are devoted entirely to an eight-bit-wide data path capable of passing one byte at a time. This transfer method is referred as "bit-parallel, byte-serial". The GPIB is bi-directional, meaning that data being sent and data being received use the same signal paths. Up to fifteen devices can be connected to the same bus, a clear advantage over other bit-serial buses commonly used like the RS-232, with which only two devices can be connected at the same time.

3.5.4. Operation sequence

Now that a general description of the instruments involved in the data acquisition system has been provided, it is necessary to explain the operation sequence involving the digitizing, storing and transferring of data.

The RTD 710 has two interfaces, the IEEE Std 488 (or GPIB) and the Direct A/D Output Port Interface. This last one allows the instrument to be used as a 10-bit, 200 megasample per second A/D converter connected to an external high-speed memory like the FDC 9503 [34].

When the RTD digitizes a signal, the binary data produced is recorded simultaneously in two places: the RTD's internal memory and the FDC memory. This is possible because of the Direct A/D Output Port Interface.

The digitizing and recording operations are initiated when an "arm on" signal is transmitted from the PC to the FDC/RTD through the GPIB. This signal arms the RTD and the FDC to start acquisition and recording of data once a true trigger level is reached at channel 1 of the RTD 710. When used in NORMAL recording mode, every new trigger level will start the acquisition of a new "record" or set of digital information, that closely represents the original analog signal.

Once all the data points of a record have been digitized, the RTD will wait until a new trigger level has been reached. Each data point is a 10-bit word of binary information, and, as mentioned earlier, the number of data points in a record are multiples of 1024 words up to 32K 10-bit words, when using the digitizer in dual channel mode, or 64K words when in "channel 1 only" mode.

The number of records that can be stored in the FDC 9503 depend exclusively on its memory capabilities. In this respect, the FDC has a very flexible memory, that consists of "segments" of 256 words in size, which indicates that its total memory of 4 Mwords consists of 16K segments. The memory size that is used in the FDC to store a record from the RTD can be equal or smaller than the size in words of the original RTD record. This is

particularly useful when not all the information in a record is required to be stored in the FDC. For example, if the valuable information from a pulse occurs within the first half of a memory record, it will be convenient to store in the FDC only that part of the record and save the other half for another pulse.

This will produce a considerable enlargement of the number of pulses that can be stored in the FDC. In general, memory management in the FDC depends on the characteristics of the pulse being digitized and on the recording mode used. It is important to note that the size of memory reserved in the FDC to store a single record has to be smaller or equal to the size in words of the record.

The number of records to be stored in the FDC are set by the user in the "time window" selection at the main menu of ASUPD. This parameter is set in the FDC, and this instrument instructs the RTD to keep digitizing pulses until the total number of records selected have been reached. The FDC halts the digitizing operation once all the required number of records have been acquired.

The PC is informed by the FDC about having in memory all the records required, and at that moment, a "collecting data loop" is initiated through software to transfer one by one the individual records from the FDC to the PC using the GPIB.

Each record received by the PC is analyzed through the following steps:

- 1) Scaling routine. The binary information is converted to an analog equivalent.
- 2) MinMax routine. The minimum and maximum voltage values contained in the record are identified.

- 3) Pulse distribution by voltage bin levels routine. The maximum voltage value is compared against voltage bin levels and a count is increased in one unit as a result of this comparison.
- 4) Charge content routine. The maximum (or minimum voltage, whichever is larger) is multiplied by a constant of proportionality in order to determine charge content of the pulse.
- 5) Pulse distribution by charge content routine. The value of charge obtained from the pulse under analysis is compared against charge bin levels, and a count is increased in one unit as a result of this comparison.

After step 5 a pulse has been completely analyzed, and the transference of a new pulse between the FDC and the PC is reinitiated. This process of transferring/analyzing will be repeated until all the pulses stored at the FDC have been successfully transmitted to the PC.

The GPIB has a transferring capability of 500 Kbytes/sec. This indicates that a 10-bit word (2 bytes) will require no less than 4 μ sec to be transferred from the FDC to the PC. If a record has a minimum size of 2 segments (512 words), the total time required to transfer it will take 2.05 msec.

3.5.5. Software

3.5.5.1. General description.

In order to provide control of the instruments and analysis of the digitized data, a program in C (ASUPD version 1.5) was specially designed for our system by TEKTRONIX Inc. in cooperation with the author. Later versions of this program (V 1.6 and 1.7), which are currently in use, were prepared by the author at ASU to further fit our particular applications. Version 1.6 provides a "manual" operating mode. Every new acquisition is activated by the user using a menu option at the PC. Version 1.7 allows an

automatic or "hands free" operating mode. The user defines the time interval between acquisitions at the beginning of the execution, and the system restarts the acquisition process automatically, without human intervention. This feature makes the system very convenient for long duration tests.

ASUPD 1.6 and 1.7 are executable files that result from the compilation of four different source programs: ASU.C, ASU2.C, ASU3.C and ASU.H. The compilation was performed using a MICROSOFT QUICK C 2.2 compiler.

Both versions of the program consist of the following parts:

1. Selection of parameters.
2. Analysis of data.
3. Presentation of results.

1. Selection of parameters.

All operating parameters of the RTD and FDC can be programmed from an IBM PC through a GPIB. For our work, it was decided to let some of those parameters be set internally in the program (invisible to the user), and the rest be selected from the keyboard through menu selections. This allows the system to be more user-friendly. The parameters that can be programmed by the user are a) peak voltage bins; b) charge bins; c) trigger levels; d) time window and e) constant of proportionality obtained in the calibration process (α).

The voltage bin levels have been set to a maximum of 20, divided in 2 ranges of 10 each, for positive and negative voltages respectively. A minimum of 2 bins per range is needed for comparison purposes.

A total of 50 bins to count charge levels has been provided. As in the case of the voltage bins, 2 charge bins are required as a minimum. The

number of bins for voltage and charge can be easily increased in the code if desired.

The digitizer has been programmed automatically in bi-slope mode. This means that two trigger levels (positive and negative) must be entered to provide a "trigger window". Any pulse that goes beyond one of the trigger levels will be recorded. A representation of this trigger mode is shown in Fig. 3.14.

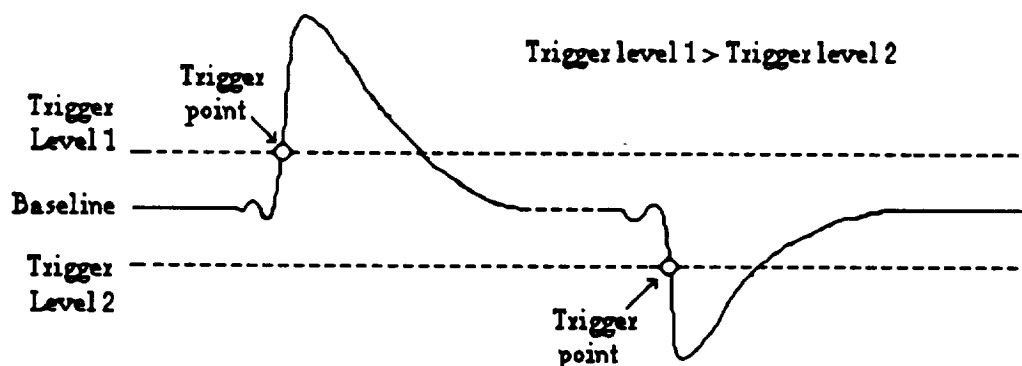


Fig. 3.14. Bi-slope triggering mode

The time window is defined as the time required for the digitizer to complete the acquisition of one record. The time window depends on 2 factors: the sampling rate and the record length. The minimum sampling time is 5 nsecs, and the smallest record size is 256 words. This creates a window of 1.28 μ secs. The size of the window can be increased by either incrementing the record length, the sampling time or both, depending on the particular application. In our system, the sampling time is automatically set to 5 nsecs, and only the size of the record can be modified by the user.

The value of a constant of proportionality alpha, as obtained in the calibration process for each particular sample under test, is entered by the

user. The process by which alpha is obtained will be explained in detail later in this chapter.

2. Analysis of data

As explained earlier, each pulse will produce an array of data in binary form that will be transferred from the FDC to the PC for analysis. This analysis consists of the following parts:

- Finding the peak value in the voltage array. Every point in the pulse array is first scaled from its original binary form to an analog equivalent. The scaling process is performed by the following C routine:

$$V_{pd} = (2 * Y_{mult}) / 1024;$$

$$V_{shift} = Y_{off} + (Y_{zero} * 5.12);$$

$$\text{for } (i = 0; i < \text{length}/2; i++)$$

$$\text{fdcwfm}[i] = (\text{fdcwfm}[i] - V_{shift}) * V_{pd}$$

where fdcwfm[i] is the data array; V_{pd} is the scaling factor of the digitizer, as discussed earlier; Y_{mult} is the voltage range of the input analog signal; V_{shift} is the scaled value of any DC component that is programmed in the digitizer (Y_{zero}) to compensate for an offset in the input signal. In the absence of an offset, $Y_{zero} = 0$, and V_{shift} will assume the value of the baseline, or analog zero, that in binary terms is equal to 512 (Y_{off} is not a variable, but a constant value of 512). In this way, all the original binary values in the data array will be converted to a signed analog equivalent. Once this step is completed, a built-in function will browse the data in the array searching for a maximum (positive or negative). This value will be assigned to the variable "max".

- Incrementing a counter in the voltage bin levels. Immediately after the peak value of the pulse has been determined, the value of max will be

compared against a list of preselected voltage bin levels. This process is performed by the following routine:

```
for ( i = 0; i <= mbl - 2; i ++ )
    if ((double) max >= maxb[i] && (double) max < maxb[i+1])
        maxs[i] = maxs[i] + 1;
```

In this routine, m_{bl} represents the total number of bin levels programmed; $maxb[i]$ and $maxs[i]$ are two arrays containing, respectively, the voltage bin levels used for comparison and the count of pulses having amplitudes between bins. Each value of max will produce the increment in one unit of only one counter, assuring in this way that each pulse will be counted only once.

- Calculating the charge content per pulse. The value of max will be multiplied by a constant α that is input at the beginning of the execution of the program. α is the result of a calibration stage, where a constant of proportionality is obtained by relating a known amount of charge, injected into the sample under test, to the amplitude of the induced pulse detected across the detection impedance R_d of the RC network. The following routine performs this calculation:

```
maxabs = fabs (max);
charge = alpha * maxabs;
```

where $maxabs$ is the absolute value of max , in case the peak value is negative.

- Incrementing a counter for charge bin levels. In the same way as in the case of the peak voltage being compared against voltage bin levels, the value of charge will be compared to preselected charge bin levels. The following routine is used for this purpose:

```
for ( i = 0; i <= ibl - 2; i ++ )
```

```

if ((double)charge >= intb[i] && (double) charge < intb[i+1])
ints[i] = ints[i] + 1;

```

where i_b represents the total number of charge bin levels; $intb[i]$ and $ints[i]$ are, respectively, arrays that represent the charge bin level values and the counter assigned to each pair of bin levels. Again, only one count will be assigned per pulse.

3. Presentation of results

Results are presented in two different ways, by displaying on the screen of the PC the peak voltage value and the charge content of each pulse immediately after it has been analyzed, and as a print-out of the total pulse distribution after the complete analysis of n records. In the first case, the information of each pulse is shown in the screen for 1 second. This time can be increased or decreased in the code depending on the user's preference (it is important to note that as this time is increased, the transfer of data between the FDC and the PC is delayed). In the case of the consolidated results, a print-out is generated immediately after the analysis of all the pulses requested has been completed. The print-out contains the following information:

- Set-up file identification
- Date and time of the acquisition
- Positive and negative voltage bins, along with their respective count values
- Charge content bins and their respective count values.

3.6. Calibration

Calibration of the system in the complete test circuit is made to determine the scale factor by which the indication of the measuring instrument (deflection in volts from normal trace in an oscilloscope), has to

be multiplied to give the desired quantity under actual test conditions with the test object connected [35]. This factor of proportionality is affected by the circuit characteristics, especially by the ratio of the test object capacitance to that of the coupling capacitor. Therefore, a new calibration factor has to be obtained for each new test object.

Calibration is made by injecting short current pulses into the terminals of the test object, as shown in Fig. 3.15, by using a square wave generator in series with a calibration capacitor C_c . As described in the IEEE 454 standard [35], the value of C_c should be smaller than C_t , normally smaller than $0.1C_t$.

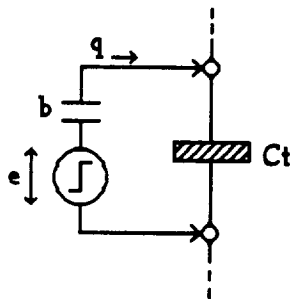


Fig. 3.15. Charge injection to sample capacitor

Two calibration modes are most commonly used, as reported by Bartnikas [2] and Kreuger [1]. These techniques are classified according to the location in the circuit where the calibration is performed. They are known as high and low voltage calibration modes. In this thesis only the high voltage calibration mode, the most accurate of the two, will be discussed. Bartnikas [2] presents a very interesting discussion about the low voltage calibration and the inherent inaccuracy associated with its practice.

3.6.1. High voltage calibration

The arrangement for this calibration mode is presented in Fig. 3.16. The square pulse generator e_c is used to inject a known charge q_c by charging calibration capacitor C_c . In Fig. 3.16, C_t = sample capacitor, C_{cc} = coupling

capacitor, C_i = detection network stray capacitance and C_s = stray capacitance across the high-voltage system.

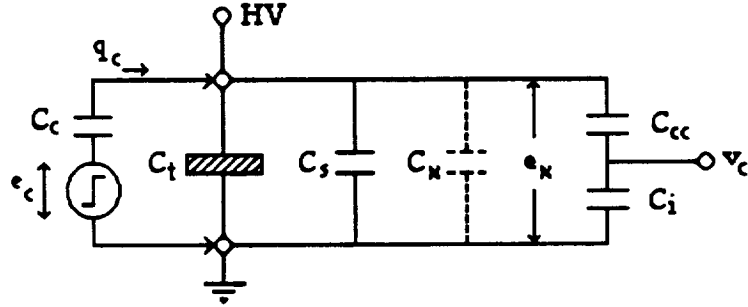


Fig. 3.16. High voltage calibration mode

The equivalent capacitance at the high voltage node, C_x , can be expressed as:

$$C_x = C_t + C_s + \frac{C_\alpha \cdot C_i}{C_\alpha + C_i} \quad (3.20)$$

and the voltage drop across this capacitance C_x , in terms of the input pulse e_c is:

$$e_x = e_c \cdot \frac{C_c}{C_c + C_x} \quad (3.21)$$

From this expression, the voltage v_c detected at the oscilloscope can be found:

$$v_c = e_x \cdot \frac{C_\alpha}{C_\alpha + C_i} \quad (3.22)$$

$$= e_c \left(\frac{C_c}{C_c + C_x} \right) \left(\frac{C_\alpha}{C_\alpha + C_i} \right) \quad (3.23)$$

$$= e_c \cdot \frac{C_c C_\alpha}{(C_c + C_t + C_s)(C_\alpha + C_i) + C_\alpha C_i} \quad (3.24)$$

$$\frac{v_c}{e_c C_c} = \frac{C_{cc}}{(C_c + C_t + C_s)(C_{cc} + C_i) + C_{cc} C_i} \quad (3.25)$$

or

$$e_c C_c = q_c = \alpha v_c \quad (3.26)$$

This value of α represents a constant of proportionality between a known charge injected into sample capacitor C_t and the amplitude of the voltage pulse across R_d . This constant depends exclusively on the particular characteristics of the detection circuit.

The calibration can be made with or without the detection network energized at high voltage. This depends on the voltage rating of the calibration capacitor. If $C_t \gg C_c$, then a very small error is involved in the calibration factor when C_c is removed from the test circuit. If the injected charge q_c is assumed equal to the charge content of an internal discharge at C_t under normal testing conditions,

$$e_c C_c = v_t C_t \quad (3.27)$$

where v_t is the voltage drop across C_t due to an internal discharge.

From equation 3.25,

$$v_c = \frac{v_t C_t C_{cc}}{(C_t + C_c + C_s)(C_{cc} + C_i) + C_{cc} C_i} \quad (3.28)$$

If the calibration capacitor is removed, this expression becomes

$$v_c' = \frac{v_t C_t C_{cc}}{(C_t + C_s)(C_{cc} + C_i) + C_{cc} C_i} \quad (3.29)$$

Therefore,

$$\frac{v_c}{v_c'} = \frac{(C_t + C_s)(C_{cc} + C_i) + C_{cc} C_i}{(C_t + C_c + C_s)(C_{cc} + C_i) + C_{cc} C_i} \quad (3.30)$$

The % error can be calculated as:

$$\% \text{ error} = \frac{v_c}{v_c'} \cdot 100 \quad (3.31)$$

it will be very small if $C_c \ll C_t$. For example, assuming the following network parameters the % error can be estimated: $C_t = 5\text{nF}$, $C_s = 200\text{pF}$, $C_{cc} = 150\text{pF}$, $C_i = 500\text{pF}$, $C_c = 100\text{pF}$, % error = 1.84%.

A simulation in PSPICE 4.04 was conducted in order to determine the expected response of the circuit to a calibration pulse applied to a sample capacitor C_t of 10nF. The calibration pulse used in this simulation, e_c , is shown in Fig. 3.17 and has the following characteristics:

- Amplitude = 7V;
- offset = 0 V;
- risetime = 50nsecs;
- frequency = 60 Hz.

The calibration circuit produces a short square pulse to across C_t . This pulse is shown in Fig. 3.18 labeled as v_i . As expected for a RC network with a time constant smaller than the time duration of the input pulse, the output pulse observed at R_d is a two-spikes waveform labeled v_c in Fig. 3.18.

3.6.2. Calibration of the test circuit

The test circuit in figure 3.2 was calibrated using a WAVETEK model 147 hf sweep generator, used as a voltage source, in series with a HAEFELY 100pF injection capacitor.

The calibration procedure was the following: the calibrator was connected across the sample capacitor as shown in Fig. 3.19, with the high voltage source deenergized.

The induced pulses v_c across R_d were observed using a TEKTRONIX 2430A digital oscilloscope.

The pulses used for calibration had a risetime smaller than 0.1μsec, as specified in the calibration pulse requirements of IEEE 454 [35].

Date/Time run: 05/14/91 12.26.08 *PD050T Temperature: 27.0

69

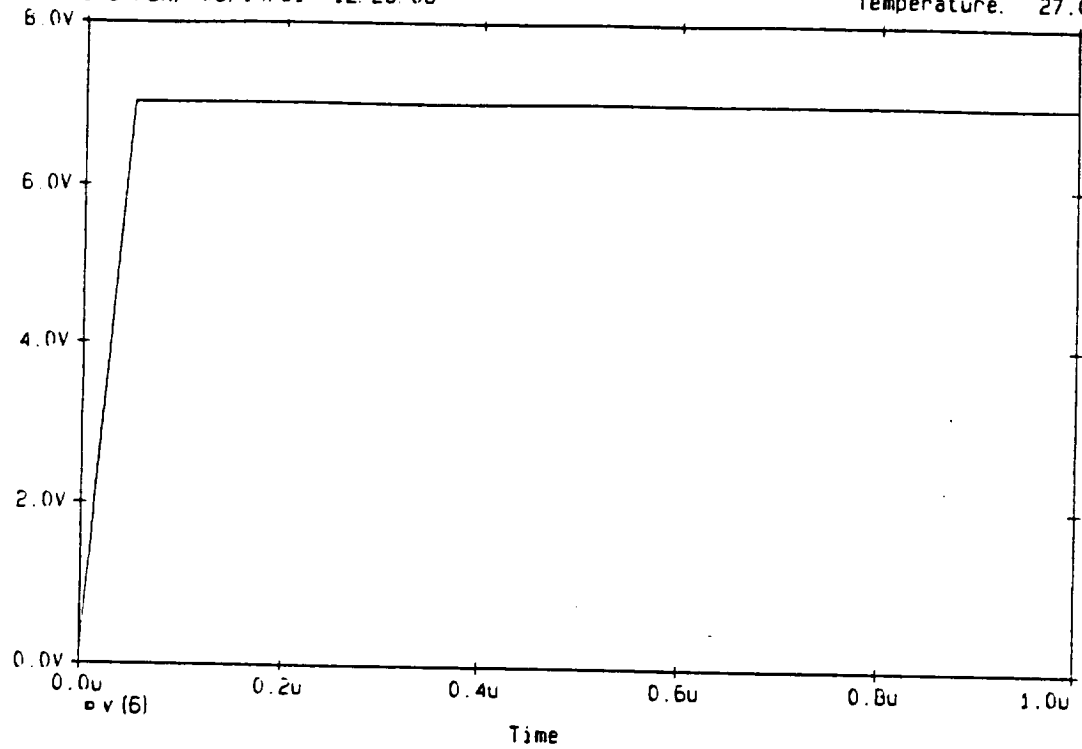


Fig. 3.17 Calibration pulse e_c

Date/Time run: 05/14/91 12.26.08 *PD050T Temperature: 27.0

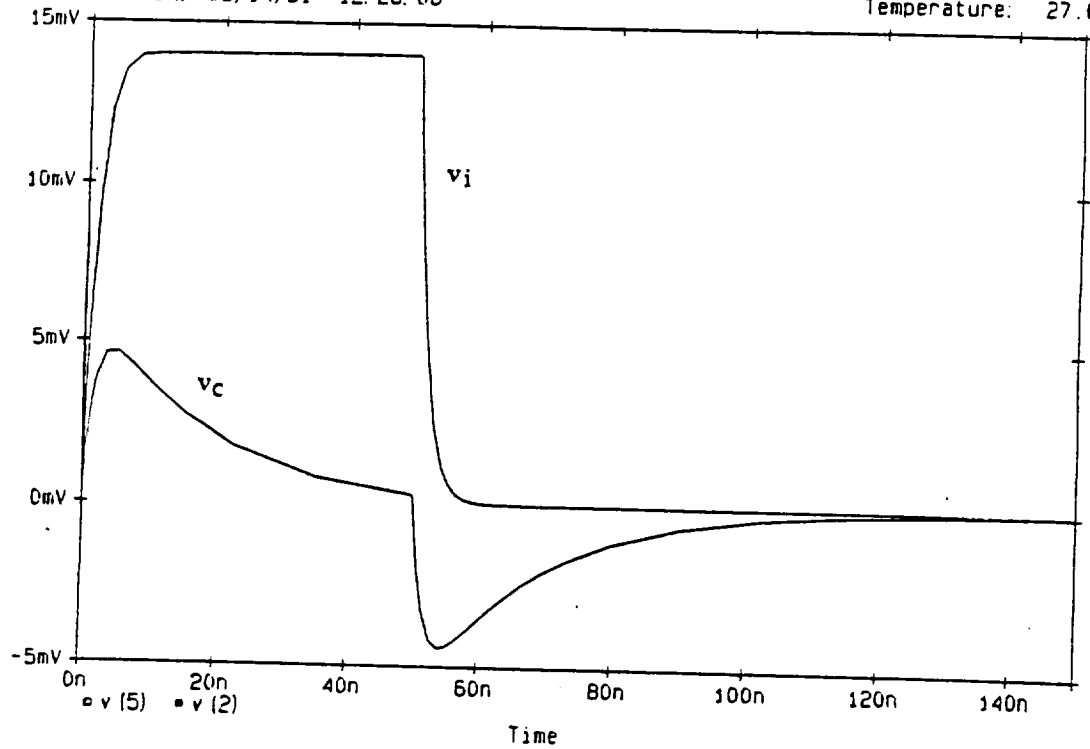


Fig 3.18 Response of the PD detection network to a calibration pulse

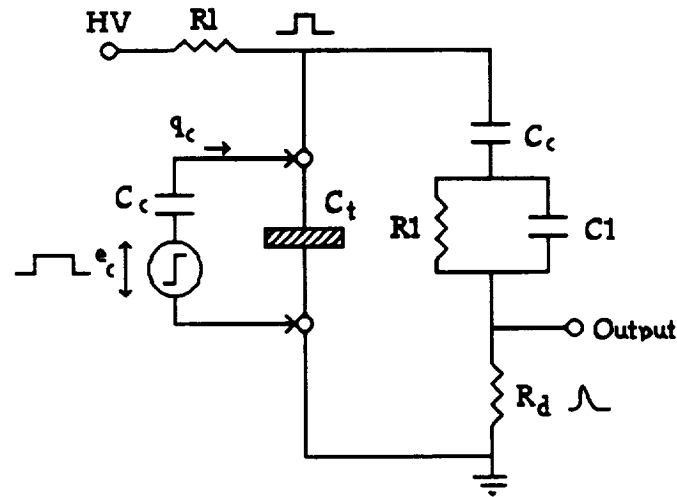


Fig. 3.19. Calibration of the test circuit

In order to calibrate the system for the test of a 1.5nF sample capacitor, a 4V input voltage e_c with a frequency of 1KHz was used to inject a charge of 400pF to C_t . The deflection produced in the oscilloscope had a peak value of 19mV. The waveforms of the calibration voltage e_c and the resulting pulse v_c are shown in Figs. 3.20a and 3.20b respectively. As can be observed, the experimental results agree with the pulse characteristics expected.

As described earlier, the output voltage v_c is related to q_c by equation 3.25, from where the value of the constant of proportionality for the sample capacitance under test can be calculated as 2.12×10^{-8} Coulombs/volt. In order to check linearity of this relationship, the calibration voltage was increased to 7V, injecting a charge of 700pC to the sample. The height of the pulse v_c obtained was 33mV, producing again a constant of 2.121×10^{-8} C/v, as in the first case.

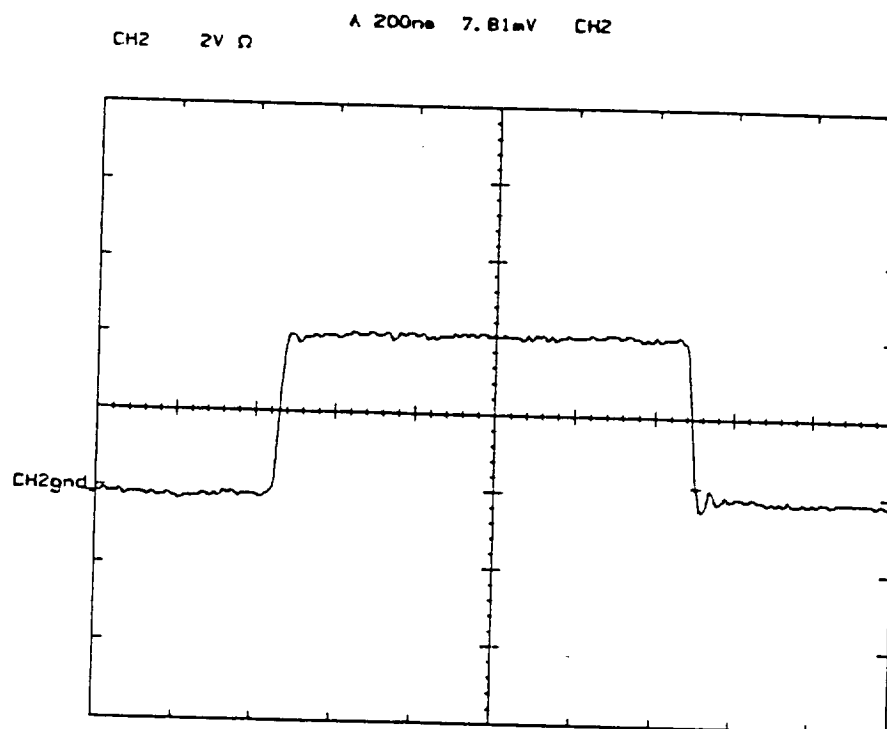
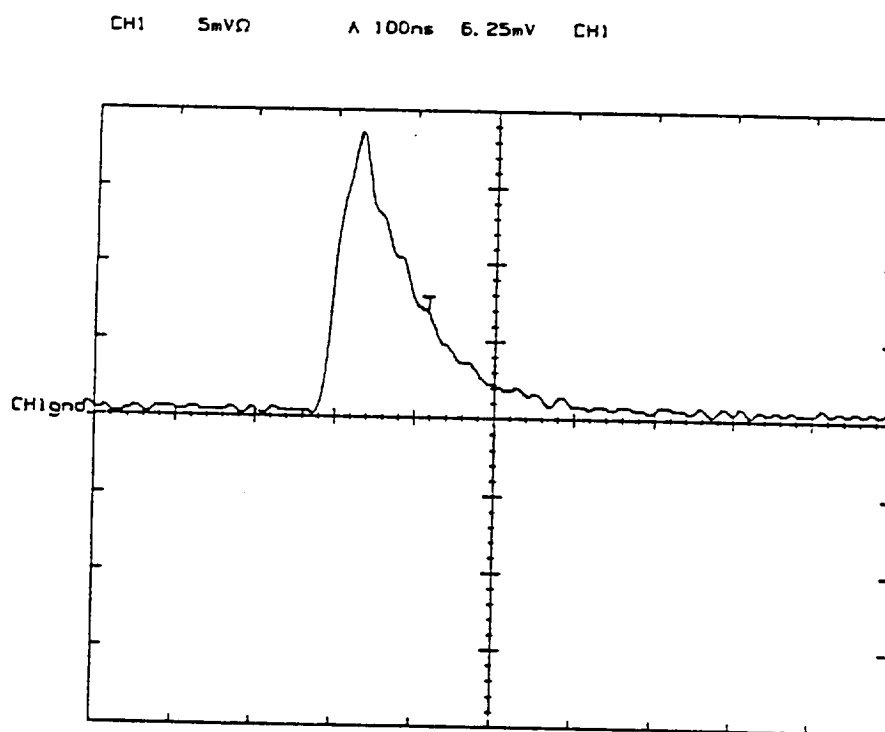


Fig. 3.20a Voltage pulse used for calibration

Fig. 3.20b Voltage v_c across R_d

PAGE INTERNATIONAL

CHAPTER 4

EXPERIMENTAL VERIFICATION

4.1. General

The overall operation of the proposed diagnostic system was tested using two different approaches: a) use of a square pulse generator directly connected to the data acquisition and analysis system; and b) testing of sample ceramic capacitors under high voltage conditions.

In the first case, a train of pulses of known characteristics was input into channel 1 of the digitizer in order to monitor the digitizing and analysis process performed by the system, and from these results evaluate the validity of the data obtained. The second case was used to evaluate the performance of the automatic version of ASUPD, by exposing sample capacitors to high voltage conditions during long duration tests.

4.2. Tests using a pulse generator.

These tests were designed to observe the digitizing process, analysis and display of information of the data acquisition and analysis system through the observation of the following characteristics:

- 1) Ability of the digitizer to capture positive and negative polarity pulses;
- 2) Storing capabilities of the Fast Data Cache;
- 3) Analysis of the data. Peak voltage detection and charge content calculation per pulse;
- 4) Distribution of pulses in bin levels;
- 5) Print-out of measurements.

Several test were carried out using a pulse generator. The results obtained were used to debug the original version of ASUPD and to produce a

program that could perform efficiently. Two of the tests will be described next.

4.2.1. Test 1

This test was carried out in order to check the ability of the program to perform the following operations:

- 1) Digitizing of positive and negative polarity pulses.
- 2) Pulse distribution according to peak values of voltage

A train of unipolar square wave pulses was input to the digitizer with the following characteristics:

Amplitude: $\pm 0.350\text{V}$, $\pm 0.750\text{V}$, $\pm 1.25\text{V}$, $\pm 1.75\text{V}$

Frequency: 650KHz

Width of the pulse: 500nsecs

Pulse generator: WAVETEK model 147 hf sweep generator

The following set-up parameters were programmed at the main menu:

Number of records: 50

Trigger levels: $L1 = 0.100\text{V}$; $L2 = -0.100\text{V}$

Bin levels for voltage: from 0V to 2V in increments of 0.5V

Fifty pulses were acquired and processed by the system in each of 4 repetitions of the experiment, using in each repetition an amplitude approximately equal to the mid-point between bin levels.

In Fig. 4.1, a print-out of each of the 4 repetitions is shown. As expected, each group of 50 pulses having the same amplitude were correctly allocated in bin levels. The test was repeated for negative pulses and comparable results were obtained.

ASU HIGH SPEED PD MEASUREMENT SYSTEM
ASUPD 1.6
TEST01

Sun Mar 10 13:14:38 1991

POSITIVE BIN LEVELS (Volts)

BINS	COUNT
0.000	50
0.500	0
1.000	0
1.500	0
2.000	0

NEGATIVE BIN LEVELS (Volts)

BINS	COUNT
-0.500	0
-1.000	0
-1.500	0
-2.000	0
-2.500	0

ASU HIGH SPEED PD MEASUREMENT SYSTEM
ASUPD 1.6
TEST01

Sun Mar 10 13:14:38 1991

POSITIVE BIN LEVELS (Volts)

BINS	COUNT
0.000	50
0.500	50
1.000	0
1.500	0
2.000	0

NEGATIVE BIN LEVELS (Volts)

BINS	COUNT
-0.500	0
-1.000	0
-1.500	0
-2.000	0
-2.500	0

ASU HIGH SPEED PD MEASUREMENT SYSTEM
ASUPD 1.6
TEST01

Sun Mar 10 13:14:38 1991

POSITIVE BIN LEVELS (Volts)

BINS	COUNT
0.000	50
0.500	50
1.000	50
1.500	0
2.000	0

NEGATIVE BIN LEVELS (Volts)

BINS	COUNT
-0.500	0
-1.000	0
-1.500	0
-2.000	0
-2.500	0

ASU HIGH SPEED PD MEASUREMENT SYSTEM
ASUPD 1.6
TEST01

Sun Mar 10 13:14:38 1991

POSITIVE BIN LEVELS (Volts)

BINS	COUNT
0.000	50
0.500	50
1.000	50
1.500	50
2.000	50

NEGATIVE BIN LEVELS (Volts)

BINS	COUNT
-0.500	0
-1.000	0
-1.500	0
-2.000	0
-2.500	0

Fig. 4.1 Print-out of results test 1

From this test it is clear that the system recognizes positive and negative pulses, and also that is capable of producing distribution of pulses according to their amplitude.

4.2.2. Test 2

In test 2, a print-out of all the elements of `fdcwfm[i]`, the array containing the pulse voltage data, was obtained for positive and negative pulses. This was done to check the validity of the routine used for scaling the binary data to its analog equivalent, i.e.,

```

Vpd = ( 2 * Ymult ) / 1024;
Vshift = Yoff + ( Yzero * 5.12 );
for ( i = 0; i < length/2 ; i ++ )
    fdcwfm[i] = ( fdcwfm[i] - Vshift ) * Vpd

```

The pulse was observed in a TEKTRONIX 2430A digital oscilloscope, in order to compare the original analog information with the one provided at the end of the acquisition process.

The characteristics of the pulse used for this test are as follows:

Amplitude: - 64mV

Frequency: 250kHz

Width of the pulse: 1μsec

Offset: +3mV

and the following parameters were set at the digitizer:

Number of records: 1

Trigger levels: L1 = 20mV, L2 = -20mV

Voltage range: 200mV

In Fig. 4.2, the waveshape of the pulse used in the test is shown in terms of both analog values and binary code.

The scaling factor, V_{pd} can be found from:

$$V_{pd} = (2 * Y_{mult}) / 1024 = 0.39mV \quad (4.1)$$

where Y_{mult} is the voltage range set at the RTD 710, i.e. 200mV.

As expected, the analog values observed at the oscilloscope matched the ones obtained after the analog/digital/analog operation performed in this test. Therefore, the system is capable of producing a string of data that closely represents the original analog pulse.

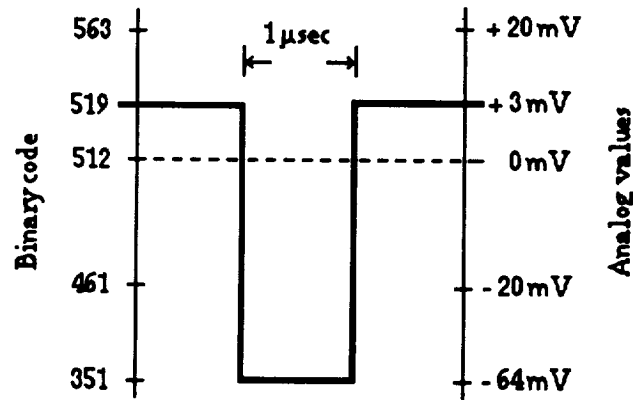


Fig. 4.2. Pulse used in test 2

4.3. Testing of sample capacitors

4.3.1. General

The proposed PD diagnostic system was fully tested using ceramic capacitors as testing specimens. In this thesis the measurements report of one of these tests is presented. The sample capacitors were tested at high voltage, approximately 25% above their corona inception voltages (CIV), for several hours until failure of the dielectric occurred. In this test, the system was programmed to acquire a sample of 500 pulses every 30 minutes, and to

produce a report of pulse distribution per voltage and charge content after the acquisition of each sample. As expected, a change in the pulse distribution per bin level of charge was observed as the dielectric aged.

4.3.2. Test set up

A 10nF, 4KV ceramic capacitor with the following characteristics was used as a test sample:

Specimen#: 8

Capacitance: 8.796 nF

Q (quality factor): 177

Z_p (impedance in parallel): $3.55M\Omega$

Z_s (impedance in series): 113Ω

D (dissipation factor): 0.005

Z (total impedance): 20.08Ω

These characteristics were obtained by measuring the capacitor with a PHILLIPS PM6303 RCL meter with a test frequency of 1KHz.

Before installing the sample capacitor, the voltage in the test circuit was raised to 10kV, and no pulse activity could be observed in the oscilloscope connected across the detection impedance R_d . The voltage was maintained at 10kV for about 10 minutes and no pulses larger than the ones noted above were observed. The sample capacitor was then installed in the test circuit as shown for C_t in Fig. 3.2.

Before starting the high voltage test, a calibration stage was required to determine the constant of proportionality needed to relate pulse height to charge content of the PD's. A WAVETEK model 147 hf sweep generator in conjunction with a HAEFELY 100pF injection capacitance were used as a calibrator for the test sample. When using a square pulse with an amplitude

of 5V, a charge of 500pF was injected into the sample. This charge produced a deflection of 8mV in the screen of the oscilloscope connected across R_d . The constant of proportionality obtained was 6.25×10^{-8} Coulombs/volt. Once the calibration procedure was completed, the pulse generator and the injection capacitor were removed from the test circuit.

The high voltage source was energized and the input voltage was gradually increased until discharges with amplitudes larger than 5mV were observed in the screen of the oscilloscope. This will be considered the corona inception voltage (CIV) of the test capacitor and corresponds to a value of 1.1KV. The voltage was further increased up to 2KV and maintained at this level for approximately 2 minutes; then it was decreased until no discharges were seen, corresponding to a voltage of 0.8KV. This voltage was considered to be the corona extinction voltage (CEV) of the test capacitor. One partial discharge captured at 2KV is shown in Fig. 4.3.

The output of the PD detection system was connected to channel 1 of the RTD 710, and at this point the system was ready to start acquisition.

The automatic version of ASUPD was loaded in the PC and the following information was requested:

- 1) Time interval:
- 2) Number of samples:

In "time interval", the program requests time in minutes between successive samples. For example, if the system is set to acquire 500 pulses/sample, the time introduced at the prompt will be the delay time the computer will wait to restart a new acquisition of another set of 500 pulses. Following the same example, "number of samples" is the total number of 500

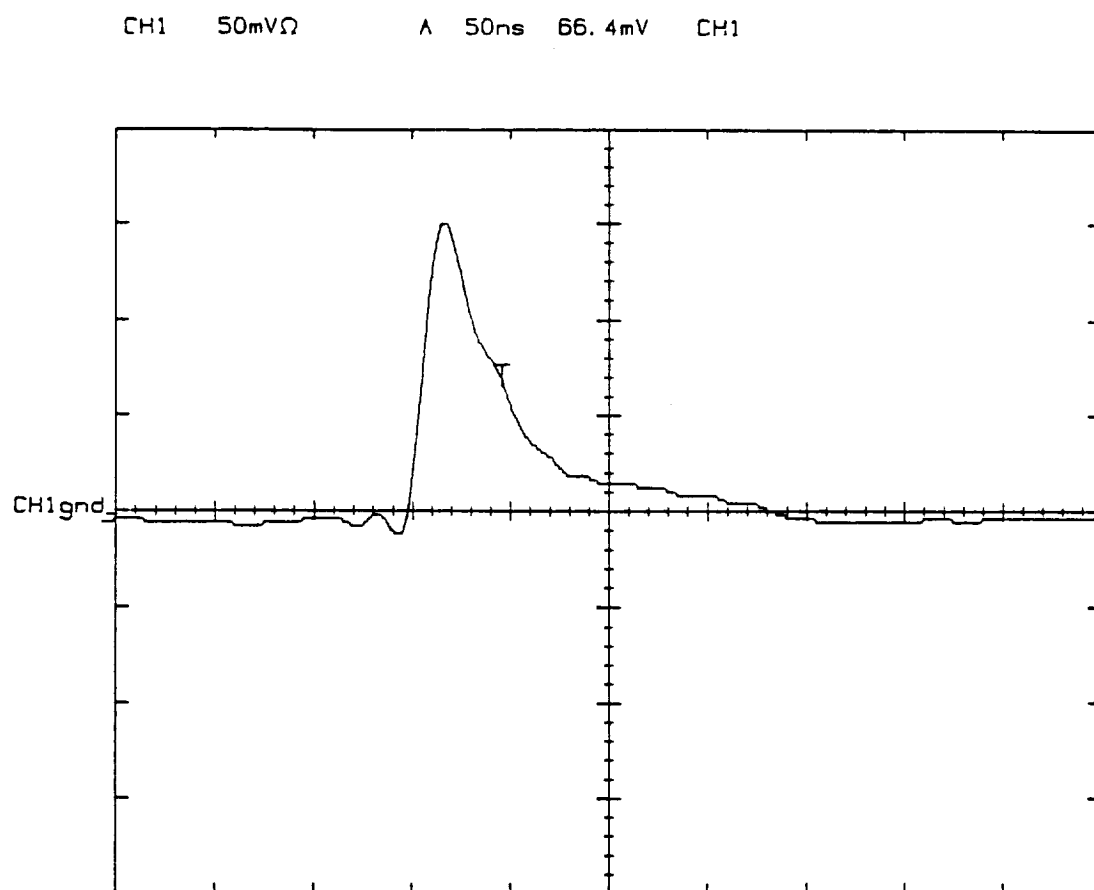


Fig. 4.3 Typical partial discharge

pulses sets that the system will acquire before halting the acquisition process. This parameter was introduced in the program to easily monitor the performance of the automatic version ASUPD, and can be removed when very long duration tests are conducted. After this information has been provided, the user can initialize the system to start acquisition.

The input voltage was then increased to 2.5kV, and the system was set to start acquisition. The sample size programmed was 500 pulses, and the delay time between samples was set to 30 minutes. A print-out of results was obtained after each sample was completely acquired and analyzed.

4.3.3. Measured results

Specimen #8 failed after 20.5 hours of continuous exposure at 2.5KV, and a total of 20,500 pulses were collected for analysis. The results of this test are presented in Figs. 4.4a and b.

The horizontal axis in these figures represents bin levels of charge from 1nC to 49nC in increments of 1nC. The vertical axis represents number of PD's per bin. These figures were constructed in the following way: the total number of pulses was divided in 6 sets, corresponding to the information contained in the reports at 500, 4500, 8500, 12500, 16500 and 20500 pulses, called S0, S1, S2, S3, S4 and S5 respectively. The differences in the number of pulses per bin levels between these reports, i.e. $S1 - S0$, $S2 - S1$, ... , $S5 - S4$, represent relative changes in pulse distribution with time, in this case 4 hours between each set. The results were plotted in two different figures due to poor resolution of the graph when all the 5 bars were plotted at the same time.

Figure 4.4a shows the distribution of partial discharges during the first 12 hours of the test, and fig. 4.4b the pulse distribution for the remaining 8 hours along with the data of the first 4 hours for comparison purposes.

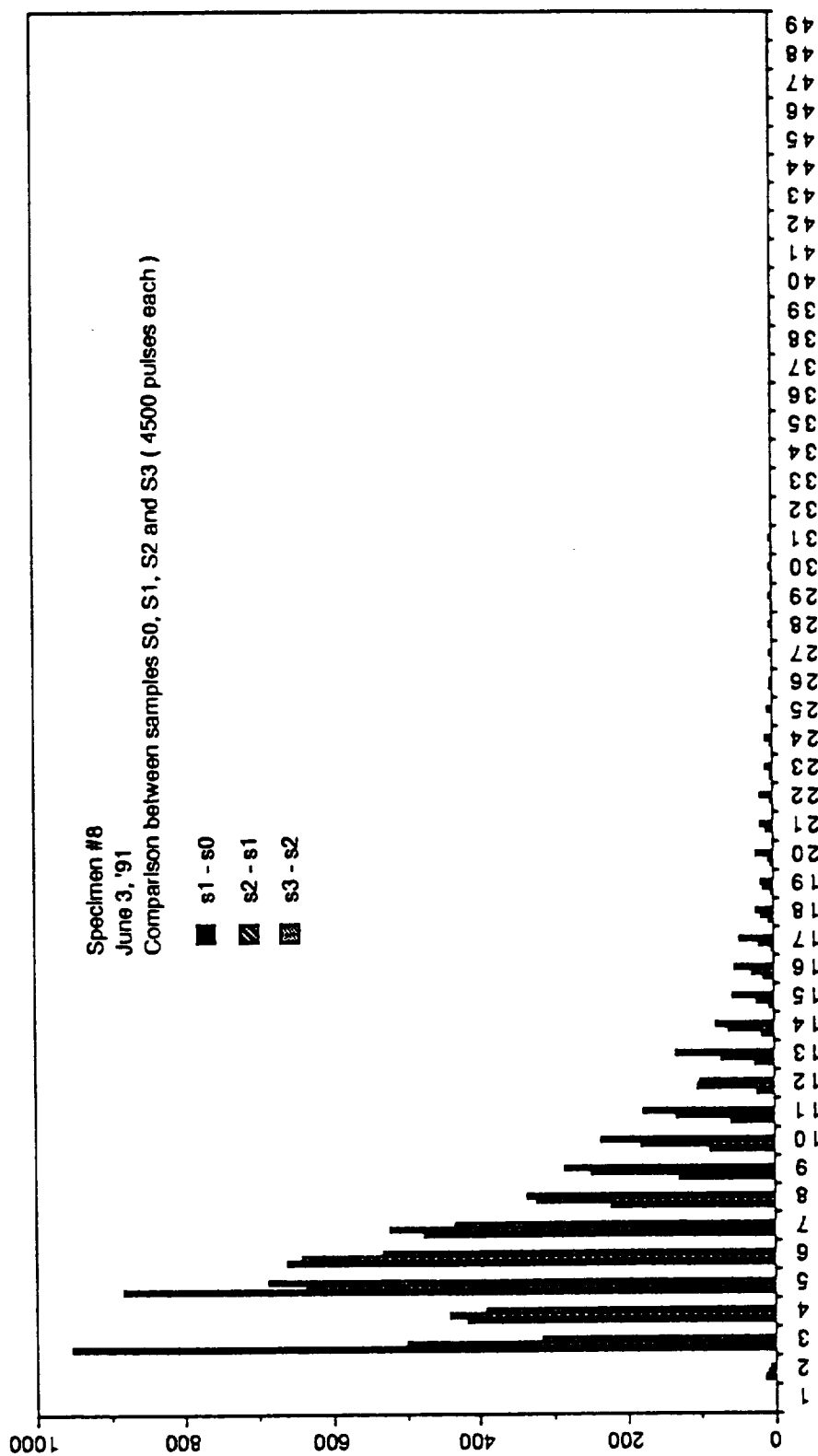


Fig. 4.4a Test results of Specimen#8: first 12 hours

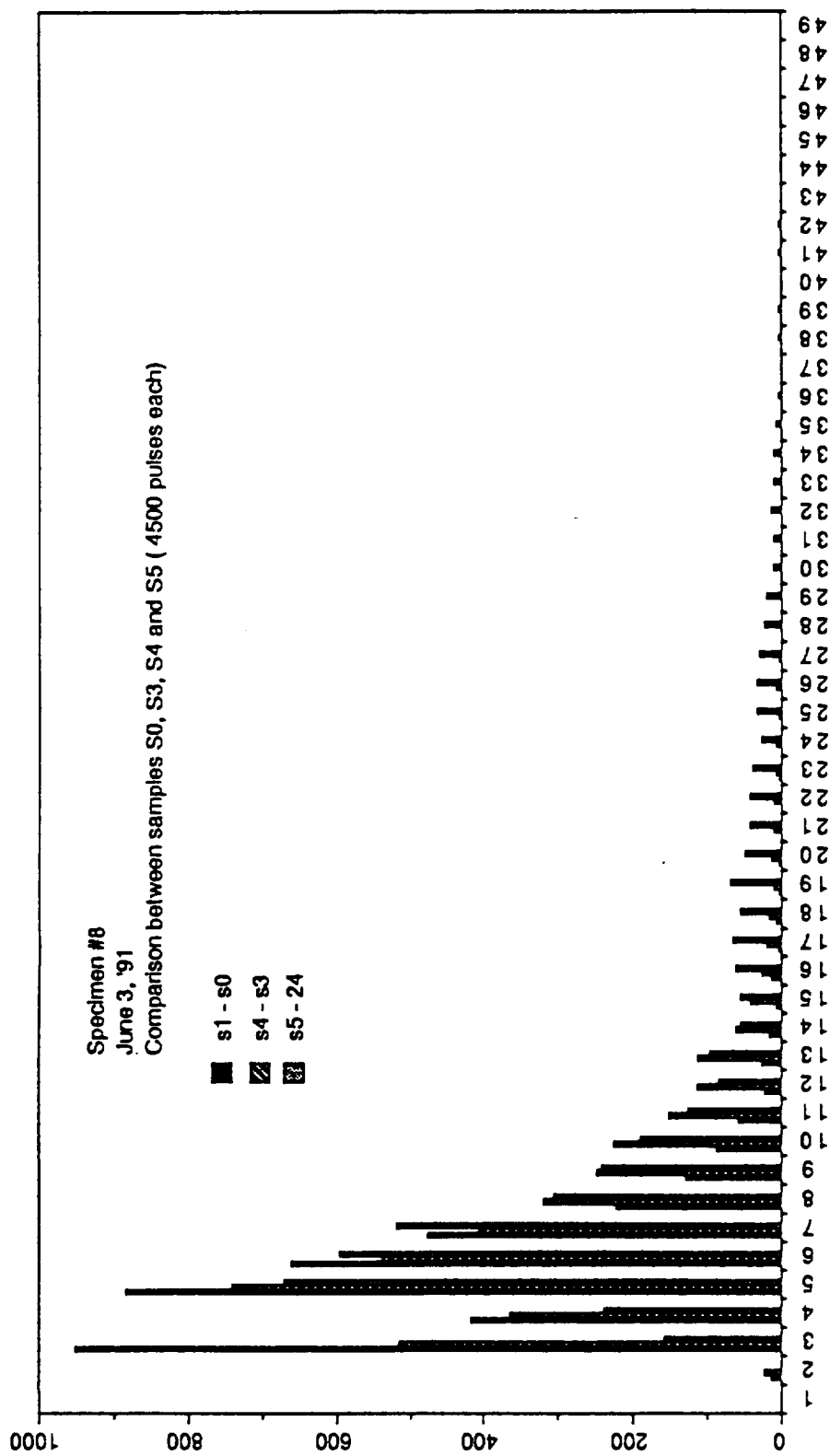


Fig. 4.4b Test results of Specimen #8: last 8 hours

As can be observed from both figures, the pulse distribution tends to shift toward higher levels of charge as the dielectric ages. These results agree with the expected behavior of capacitors under long duration tests as reported by Dunbar [36].

One of the characteristics observed during this test was the production of heat by the PD's in the dielectric material of the capacitor.

In order to correlate rise in temperature with presence of partial discharges, a thermocouple was placed on the surface of the capacitor, and the temperature was observed with a FLUKE 75 digital voltmeter using a FLUKE 80TK thermocouple module transducer. Temperature readings were obtained for three different values of input voltage. After each voltage level was reached, it was maintained constant for 5 minutes and at the end of this time the temperature reading was obtained. Although this short experiment is not directly related to the use of the PD diagnostic system, the author found interesting results than assure that the discharges detected for the system were in effect produced inside the capacitor. The results from this experiment are the following:

Voltage (KV)	Temperature (°F)	Comments
0.76	87.2	No discharges are present. Reading indicates room temp.
1.37	91.5	Small discharges with amplitudes no larger than 25mV were observed.
2.0	106.6	Discharges with amplitudes up to 300mV were observed.

4.4. Conclusions from the measured results

From the testing with the pulse generator and the sample capacitors, the following conclusions can be made about the measured results:

- 1) The proposed PD detection system is capable of recognizing pulses with either positive and negative polarity and producing a distribution of pulses according to peak voltage and charge content.
- 2) The analog information of a signal is successfully converted to digital code for digitizing and storing purposes and can be recovered again as analog data for analysis. The digitizing rate will determine how well an analog signal can be represented by a digital string of data.
- 3) The system successfully performs long duration tests using the automatic version of ASUPD. No supervision is needed once the acquisition process has started, making the system very convenient for long duration testing.
- 4) The information provided by the system is very easy to correlate, and produces valuable data for the study of the degrading mechanisms in dielectrics due to partial discharges.
- 5) The distribution of pulses according to their charge content, shifts to higher levels of charge as the dielectric ages.
- 6) Partial discharges produce a rise in the temperature of the material under test, and this temperature is directly related to the level of discharges occurring inside the material.

PAGE _____ INTENTIONALLY BLANK

CHAPTER 5

CONCLUSIONS AND RECOMMENDATIONS FOR FUTURE WORK

A new concept in the measurement and analysis of partial discharges has been implemented. The use of a 200Msamples/sec. real-time waveform digitizer in conjunction with a fast memory unit has produced an extremely flexible PD diagnostic system that have been succesfully tested under normal high voltage test conditions.

Ceramic capacitors with capacitances in the range of 1nF to 10nF were exposed to high voltage in long duration tests, and the insulation life of one of them was closely monitored by sampling internal discharges in a period of 20.5 hours. The results of these tests demonstrate the ability of the PD diagnostic system to acquire and analyze internal discharges within capacitors under test, by producing valuable data that can be used to get a better understanding of the degrading mechanisms of partial discharges in dielectric materials.

5.1. Conclusions

From the experimental results in long duration tests, the following conclusions can be inferred:

- 1) Partial discharges produce gradual degradation of insulating materials. This degradation depends strongly on the exposure time and on the magnitude and frequency of the applied voltage.
- 2) The charge content of the partial discharges tends to shift toward higher levels of charge as the dielectric ages. This was observed by an increased in the amplitude of the discharges with time of exposure.

- 3) The PD diagnostic system proposed was able to record large number of pulses during long duration test of capacitors, and produce a statistical pulse distribution by peak voltage and charge content.
- 4) The information obtained from these tests was used to correlate time of exposure with charge content of the pulses. As expected, a shift in the charge content of the partial discharges with time of exposure was observed.
- 5) Partial discharges produce a rise in temperature of the dielectric under test. Although this rise in temperature cannot be directly correlated to the magnitude of the discharges, it provides a rough indication of the presence of discharges inside the material.
- 6) The performance of the PD detection system was improved by a modification in the characteristics of the output impedance. As can be observed by comparing Figs. 3.3 and 3.8, better frequency response of the detection circuit was achieved by replacing the output impedance by a cascade set of three high-pass RC filters. The higher output impedance in this modification was successfully matched to the low input impedance of the measuring instrument by a 100MHz buffer amplifier.
- 7) The modification of the detection impedance in the PSF affected not only the pulse resolution but also the level of attenuation of the power voltage. This increment in attenuation allows an increased in the sensitivity of the PD diagnostic system.
- 8) The system requires no pulse "pre-shaping" stage, as needed for Multichannel analyzers. Due to the fast digitizing rate of the RTD710, pulses can be input directly from the detection impedance to the acquisition system.

The flexibility of the system can be further exploited to produce more information about the behavior of the discharges under different test conditions.

5.2. Future work

The author proposes the following recommendations for additional work that can be done using the PD diagnostic facility:

- 1) Modification of the actual program (ASUPD) to provide a second input channel in the RTD 710 for the measurement of the applied voltage. In this way, if a discharge and the instantaneous value of the applied voltage at which the discharge occurs can be acquired almost simultaneously, measurements of energy levels of the PD's can be accomplished.
- 2) Optimization of the program in order to reduce execution time for the analysis of each pulse.
- 3) Addition of graphics capability to the program, specifically in the form of a histogram. A graphics routine to represent changes in pulse distribution with time of exposure after each data print-out could significantly reduce the analysis time of a specimen material.
- 4) Design of new testing set-ups for capacitors. a) Test of the capacitors at power frequencies higher than 60Hz, specifically at 20KHz. This experimentation is required to test dielectric materials for aerospace applications using high frequency power sources; b) Specimen capacitors exposed to a rise in temperature by artificial means. This experiment could

provide interesting results by observing possible changes in the behavior of the charge distribution of PD's as the temperature of the surrounding medium rises.

5) Improvement of the detection network response. It has been demonstrated that a change in the detection impedance for a cascade of RC high-pass filters introduces an improvement in the pulse shape and sensitivity of the system. The author suggests considering the possibility of replacing the 50Ω detection impedance by a high-pass active filter, using broadband ($> 100\text{MHz}$) operational amplifiers.

5.3. Contributions

The following list presents the contributions provided by the author in performing the research work presented in this thesis:

1. Designed and developed a fast computer-based PD diagnostic system to be used in long duration tests.
2. Conducted preliminary experimental work in order to relate PD charge content with dielectric degradation.
3. Designed a new PD detection network using a series of RC high-pass filters as detection impedance.

REFERENCES


- [1] F. H. Kreuger, Partial Discharge Detection in High - Voltage Equipment, London: Butterworths, 1989.
- [2] R. Bartnikas, Engineering Dielectrics vol 1, Corona Measurements and Interpretation, ASTM: Philadelphia, 1979.
- [3] Electrical Power Research Institute, Transmission Line Reference Book, 345 kV and Above". Palo Alto: EPRI, pp. 169-171, 1987.
- [4] G. Karady, M. D. Sirkis, L. Liu, "Investigation of High Altitude Corona Initiation Voltage", Seventh International Symposium on High Voltage Engineering. Dresden, Germany, August 26-30, 1991.
- [5] S. A. Boggs, "Partial Discharge - part III: Cavity induced PD in Solid Dielectrics", IEEE Electrical Insulation Magazine, Vol 6, No. 6, pp. 11-20, 1991.
- [6] E. Kuffel and W. S. Zaengl, High Voltage Engineering Fundamentals, London: Pergammon Press, 1984.
- [7] R. T. Harrold and T. W. Dakin, "Ultrasonic Sensing of Partial Discharges within Microfarad value AC capacitors". IEEE transactions on Power Apparatus and Systems, vol. PAS-98, No.2, pp. 444-448, 1979.
- [8] T. M. Bilodeau, "The Development of the New High-speed Partial Discharge Diagnostic System to Study Transient Electrical Failure Mechanisms in Capacitors", Ph. D. thesis, SUNY at Buffalo, 1987.
- [9] G. Garcia and B. Fallou, "Equipment for the energy measurement of partial discharges", Proceedings 1st. International Conference on Conduction and Breakdown in Solid Dielectrics, Conf. Record 8CH 1836 - 6 - EZ, Toulouse, France, pp. 275-281, 1983.

- [10] C. Menguy, Ph. Guerin, B. Fallou and D. Fortune, "Partial Discharge Energy Measurements on Insulation Systems and Equipments", Conf. Record of the 1988 IEEE Intl. Symposium on electrical Insulation, Boston, Ma, pp. 258-261, June 1988.
- [11] J. Lynch, "Partial Discharge Testing using the Pulse Height Analysis", IEEE Trans. on electrical Insulation, pp. 65-78, 1982.
- [12] S.A. Boggs, "Partial Discharge - Part I : Overview and Signal generation", IEEE Electrical Insulation Magazine, Vol. 6, No. 4, pp. 33-39, 1991.
- [13] J.H. Mason, "Discharges", IEEE Trans. on Electrical Insulation, Vol. 13, No. 4, pp. 211-238, 1978.
- [14] J.P. Steiner, "Partial Discharge - Part IV : Commercial PD Testing", IEEE Electrical Insulation Magazine, Vol. 7, No. 1, pp. 20-32, 1991.
- [15] CAMBERRA Nucler Products Group, Product Catalog, Edition Eight, Meriden, CT, 1990.
- [16] Hewlett Packard, Model 3712A Correlator Field Training Manual, U.K., 1970.
- [17] S.A. Boggs, G.L. Ford and R.C. Madge, "Coupling devices for the Detection of Partial Discharges in Gas-Insualted switchhhhgear", IEEE Trans. on PAS, Vol. 100, No. 8, pp. 3969-3973, 1981.
- [18] S.A. Boggs, "Partial Discharge - Part II : Detection Sensitivity", IEEE Electrical Insulation Magazine, Vol. 6, No. 5, pp. 35-42, 1991.
- [19] F.H. Kreuger, Discharge Detection in High - Voltage Equipment, London: Butterworths, 1965.
- [20] L. Jones and A.F. Chin, Electronic Instruments and Measurements, New York: John Wiley & Sons, 1983.

- [21] I.A. Black, "The Pulse Discrimination System for Partial Discharge Measurements in Electrically Noisy environments", BEAMA Conf., pp. 300-308, 1978.
- [22] G.H. Vaillancourt, A. Dechamplain and R. Malewski, "Simultaneous Measurement of Partial Discharge and Ratio-Interference Voltage", IEEE Trans. on Instrumentation and Measurement, Vol. 31, pp. 49-52, 1981.
- [23] T.W. Dakin, "The Relation of Capacitance Increase with High Voltage to Internal Electric Discharges and Discharging Void Volume", Trans. AIEE IIIA, Vol. 78, pp. 790-795, 1959.
- [24] A. Kelen, "Critical Examination of the Dissipation Factor Tip-Up as a Measure of Partial Discharge Intensity", IEEE Trans. on Electrical Insulation, Vol. EI-13, No. 1, pp. 14-23, February 1978.
- [25] W.P. Baker, Electrical Insulation Measurements, Newnes Intl. Monographs on Electrical Engineering and Electronics, 1965.
- [26] P.J. Harrop, Dielectrics, London: Butterwoths, 1972.
- [27] HAEFELY Partial Discharge Detector 561, Operating Instruction Manual, HAEFELY Test systems, Inc., Woodbridge, VA, 1985.
- [28] H.H. Chiang, Electronic Waveforming and Processing circuits, New York: John Wiley & Sons, 1986.
- [29] A.J. Schwab, High - Voltage Measurement Techniques, Cambridge: MIT Press, 1972.
- [30] DATEL Data Acquisition and Conversion Handbook, General Electric, Mansfield, Massachusetts, 1979.
- [31] TEKTRONIX, Inc., Product Catalog 1990, TEKTRONIX, Inc., Beaverton, Oregon, 1989.

- [32] RTD 710 Digitizer Instruction Manual, TEKTRONIX, Inc., Beaverton, Oregon, 1987.
- [33] GPIB User's Resource Utility for the IBM Personal Computer, GURU II, TEKTRONIX, Inc., Beaverton, Oregon, 1987.
- [34] R. Meketa, Applications Engineer, TEKTRONIX, Inc., Albuquerque, NM, Personal communication, 1990-1991.
- [35] IEEE Recommended practice for the detection and measurement of Partial Discharges. IEEE Standard 454-1973.
- [36] W.G. Dunbar, "Designing and Building High Voltage Power Supplies", AFWAL - TR - 88 - 4143, Vol. 2, Materials Laboratory, WPAFB, Ohio, pp. 164-167, August 1988.

CLASSIFICATION

		Report Documentation Page	
1 Report No NASA CR- 189057	2 Government Accession No.	3 Recipient's Catalog No.	
4 Title and Subtitle Design of a Fast Computer-Based Partial Discharge Diagnostic System		5 Report Date August 1991	
		6 Performing Organization Code	
7 Author(s) Jose R. Oliva, G.G. Karady and Stan Domitz		8 Performing Organization Report No. None	
		10 Work Unit No.	
9 Performing Organization Name and Address Arizona State University Department of Electrical Engineering Tempe, AZ 85287-5706		11 Contract or Grant No. NAG3-1139	
		13 Type of Report and Period Covered Contractor Report Final	
12 Sponsoring Agency Name and Address National Aeronautics and Space Administration Lewis Research Center Cleveland, Ohio 44135-3191		14 Sponsoring Agency Code	
15 Supplementary Notes			
16 Abstract <p>This paper describes a new computer-based partial discharge diagnostic system that has been successfully tested in the laboratory by performing long duration tests on dielectric materials. The system uses a 200 Megasamples/sec real time waveform digitizer in conjunction with a fast memory unit and a personal computer in order to obtain a close digital representation of a partial discharge. The digital data obtained can be easily manipulated for further analysis. This system is capable of recording large number of pulses without dead time and producing valuable information related to amplitude, polarity and charge content of the discharges. The operation of the system is automatic and no human supervision is required during the testing stage. Long duration tests of ceramic capacitors were performed in order to validate the operation of the diagnostic system. The results obtained agree with the experimental data of other researchers. From the measured results it was evident that the statistical distribution of partial discharges shifts toward higher levels of charge as the deterioration in a sample capacitor increases. The system is particularly suitable for aging studies on dielectric materials under different test conditions.</p>			
17 Key Words (Suggested by Author(s)) partial discharges, diagnostic systems, real time digitizer, fast data cache, General Purpose Interface Bus (GPIB), automatic operation		18 Distribution Statement Unclassified, Unlimited Subject Category	
19 Security Classif. (of this report)	20 Security Classif. (of this page)	21 No of pages	22 Price*
"NATIONAL SECURITY INFORMATION" Unauthorized Disclosure Subject to Criminal Sanctions.		CLASSIFIED BY: _____ DECLASSIFY ON: _____	
WHEN SEPARATED FROM ENCLOSURES, HANDLE THIS DOCUMENTATION PAGE AS: _____			

CLASSIFICATION

Page 100